Modeling Directional Interactions in Classical Molecular Dynamics for Geometrical Aspects of Nanostructures

Suhail Lubbad

Department of Physics and Technology
University of Bergen
June 2009

Thesis submitted in partial fulfillment of the
requirements for the PhD degree

Preface

I shall like to express deep thanks to professor Ladislav Kocbach for a constructive and instructive supervision and collaboration. Special thanks are also forwarded to professor Jan Petter Hansen and all colleagues in atomic and optics group at the Department of Physics and Technology, University of Bergen, Norway.

Mother, brothers and sisters
You have been and are sourcing me a strong, words are functionless to depict mine mental feelings, emotional thoughts, intellectual rationality nor emotion towards you.

Late father and oldest brother
You have sourced parts of me(s) so many times apart before leaving me behind, such I(s) stay deeply in what I have been, what I am and what I will all times be, the very same I(s) will be visioning you every-when in a time reversal around.

Friends in Bergen
Thanks for being my potential strength to go over difficulties in living.

Bergen, June 2009

Suhail Lubbad

Contents

Chapter 1

Introduction

Our aim throughout this project has been to understand and possibly improve the ways in which the classical molecular dynamics (MD) can incorporate geometries and shapes of different structures. The areas of knowledge mostly belonging to the field of chemistry were originally very little known to us, but we had some knowledge of solid state physics and atomic and molecular physics, fields which are closed to the main research fields of our Department. The first period of this project some years ago has been connected with the so called Tersoff potential. The meaning of the words "Tersoff potential" will become clear later, it is simply one of several known model interactions suitable for silicon and carbon. Carbon nanostructures, in particular possible understanding of the conditions under which carbon nanocones would be preferred over carbon nanotubes has probably been the first motivation of studying the Tersoff potentials.

Originally, MD simulations of composition of different nanostructures were the plan for the research. using the MD software package PROTOMOL, developed partly here in Bergen. However, the implementation of Tersoff's interactions in the PROTOMOL package was not at all straightforward. Thus we started to study the potentials themselves, why are they designed in their present form and in principle how one can really simulate chemistry with the help of classical potentials. This has then become the present subject of this research. In the thesis I will come several times to this important relation between classical and quantum approaches, simply expressed by the statement that chemistry can really be understood only from the quantum point of view.

In the generally known presentations of atomic interactions one usually meets interactions between two particles, which are naturally called two-body interactions or pair interactions. Further, the most known interactions depend only on the distances between the two partners, the word is isotropic, no angles are involved. To explain complicated structures as for example the famous diamond structure or the shape of the fullerenes, it is necessary to go

beyond two-body isotropic interactions. It has been found that interactions which describe the spatial structures can be thought of to be derived from sort of series expansions of the so called potential energy surfaces for the system of particles. Such a series can be interpreted as a sum of two-body, three-body, four-body etc potential functions. The first such approach we know about is the work of Axilrod and Teller already in 1943, but the work of Stillinger and Weber from 1985 is closer related to the discussion, since they explicitly described the series expansions. The tersoff potential mentioned above can also be seen in the same line of research. The two-body potentials control the mutual distances between pairs of atoms, also known as bond lengths. The angle between two bonds involves a triplet of atoms and so can be described only by three-body potentials. The spatial correlation of four particles involving three bonds is specified in chemistry by so called dihedral angle. For many readers this can be simply said as the angle between the two planes formed by the two closest triplets in the quadruplet in question, and this can be described by four body potentials. The question to be raised is "when can we stop?". Stillinger and Weber stopped at the three-body term, Tersoff left the idea of the expansion, but effectively remained also at the three-body level.

The just described paradigm of molecular modeling is probably not the most known one. More often molecular dynamics or molecular mechanics refers to studies where most of the bonds are unbreakable. The models of chemical compounds or other groups of atoms are parts of the model. Together with a large collection of empirical chemical knowledge are in these cases parts of so called force fields. The most famous are probably AMBER and CHARMM, also with very powerful molecular dynamics software, optimized for the use in several fields of research, mainly in biosciences. The present work is part of a different branch of molecular modeling, where the formation of structures and bonds is of prime interest, and our work is more related to material research and condensed matter physics. However, these areas of research share many features and a differentiation between them is probably not generally useful. Nevertheless, the term "molecular mechanics" is becoming more popular recently. In my work I have had great use of literature which could be classified more as molecular mechanics while our research belongs to the molecular dynamics area.

The investigation of atomic interactions led us to the design of our own molecular dynamics software which has been in later stages implemented mostly using the computing and visualization system MATLAB. Work with these aspects has been a large part of my project. Visualization of the geometrical structures inside MATLAB, as well as the two free systems, VMD and JMOL has contributed to our understanding of the problems and results. In visualization, we have also learned that not all tasks are best done with computers. I have rediscovered the molecular model building sets which gave the possibility to grasp

some three-dimensional relations much faster than any computer programs would allow at present without any expensive 3-dimensional visualization equipment.

The analysis of the existing models has shown that the Tersoff type potentials could be modified, but especially to a conclusion that there might be a place for a new approach. A very successful and complete interaction model called ReaxFF (Reactive Force Fields) is becoming more and more popular. However, unlike the earlier models, the ReaxFF contains many parameters and is indeed very complex. We have instead tried to design one more model which is in principle very simple and intuitive, but will allow inclusion of many parameters to improve the fitting of the known chemistry. We have called this model Orbital Based Molecular Dynamics (OBMD). The new idea is that the structure is not represented by the potential, but is a part of the interacting objects, model of atoms and their orbitals. As a result, all the necessary potentials become pair interactions.

The work on this project resulted in five distinct papers which are included in the thesis in chapter 7.

Chapter 2

Theoretics and Contemplation

In this chapter we shall look at some basic features of classical mechanics, quantum mechanics and statistical physics. The stability of matter and the basic understanding of chemistry are only possible in the quantum perspective. Nevertheless molecular modeling is based on classical Newton equations. We discuss in some detail these matters.

Many applications of molecular simulations are concerned with systems of finite temperature. Thermodynamics and its microscopic basis - statistical mechanics are thus essential in many applications. In this chapter we thus also look at some features of the statistical mechanics, especially at the implications of the so called ergodic theorem.

The topics covered in this chapter can be found in various textbooks, but the discussions in section 2.2.1 are based to some degree on an advanced research review and are generally not found in introductory texts.

2.1 Newtonian mechanics and quantum mechanics

When matter is viewed as collection of atoms, classical physics can not explain the stability of matter. Chemical properties of materials and stability of matter follow only from quantum mechanics.

In classical "Newtonian" mechanics for a collection of bodies one seeks to find all their positions and motions as a function of time. The positions are given by coordinates X(t) which obey newtons equations, given as a collection of ordinary differential equations For N objects the vector X contains 3 times N components,

$$M\ddot{X} = -\nabla V(X) \tag{2.1}$$

and the starting velocities $\dot{X}(t_0)$ must be specified at one time t_0 M is a generalized mass

matrix, ∇ specifies the 3-N dimensional gradient. As is well known, this gives us trajectories for all N particles, it means $X(t)$ and $\dot{X}(t)$ for all times. In other words, if at one instant of time the position and momentum of each particle in a system are known, then all trajectories at any later as well as earlier times are precisely computable by integrating the corresponding Newtonian equations of motion. The evaluation of forces from potentials as implied by the gradient and vice versa is not possible for all types of interactions. Alternatively, one can use the mathematical generalizations via the so called Lagrange and Hamilton formulations. These are built on mathematical theorems for systems of ordinary differential equations and allow treatment of much more general types of interactions (see also section 2.2.1).

Thus Newtonian world consist of interacting bodies with conserved total energy and trajectories in principle determined for all times, if completely known at one instant of time. This classical world-view was well described by the French mathematician Pierre Laplace:

> "An intelligence which at a given instant knew all the forces acting in nature and the position of every object in the universe - if endowed with a brain sufficiently vast to make all necessary calculations - could describe with a single formula the motions of the largest astronomical bodies and those of the smallest atoms. To such an intelligence, nothing would be uncertain; the future, like the past, would be an open book."

Classical theory of mechanics can neither determine nor explain physics at scales of the atomic and molecular systems.

Quantum mechanics uses the same set of coordinates for the position of the interacting bodies as classical equations 2.1 , but no deterministic equations for trajectories exist as in classical mechanics. Instead, equations must be found and solved for time development of so called wavefunction or state vector. These Schrödinger wave equations are constructed as hamiltonian equations of motion, but the physical quantities themselves are replaced by so called operators. The relations connecting the operators, which can be e.g. operators of differentiation is applied to the unknown wavefunction, giving the differential equation of Schrödinger. For most systems of interest the Schrödinger equations are well known. For illustration we show the Schrödinger equation for a one-dimensional motion. The coordinate is x, the momentum operator $p_x$and the total energy operator E

$$p_x = -i\hbar\frac{\partial}{\partial x} \qquad\qquad E = i\hbar\frac{\partial}{\partial t} \tag{2.2}$$

and the relation $E = p_x^2/2m + V(x)$ then gives the Schrödinger equation

$$-\frac{\hbar^2}{2m}\frac{\partial^2}{\partial x^2}\Psi(x,t) + V(x)\Psi(x,t) = i\hbar\frac{\partial}{\partial t}\Psi(x,t) \tag{2.3}$$

This so called time-dependent Schrödinger equation (TDSE) is much less known than the time independent version. This appears as a consequence of separation of variables, assuming that the solutions are of the form $\Psi(x,t) = \psi(x)\varphi(t)$, giving solutions of the type

$$\varphi(t) = \exp(-\frac{i}{\hbar}Et) \tag{2.4}$$

and the remaining time-independent or stationary equation

$$-\frac{\hbar^2}{2m}\frac{\partial^2}{\partial x^2}\psi(x) + V(x)\psi(x) = E\psi(x) \tag{2.5}$$

The importance of these stationary states follows from the probability density interpretation of the wavefunction, i.e. that the only information obtainable is the probability distribution of the studied coordinate,

$$\rho(x,t) = |\Psi(x,t)|^2 \tag{2.6}$$

Since the time component $\varphi(t)$ is in fact only a phase factor with absolute value one, the so called stationary solutions give stationary probability density (i.e. independent of time)

$$\rho(x) = |\Psi(x)|^2 \tag{2.7}$$

Solutions of equation 2.5 are only possible for certain values of the constant E, giving the energy spectrum of the system in question. The detail treatment of this formulation can be found in every introductory quantum mechanics or quantum chemistry text.

The probability interpretation of equation 2.6 has been postulated by Max Born in 1926 (in a footnote) and gave him a Nobel prize only as late as 1954. When the $\rho(x)$ is known and the quantity x is measured, the relative probability of obtaining the result $x_0 \pm \Delta x$ will be given by

$$\Delta P(x) = \rho(x)\Delta x \tag{2.8}$$

This interpretation is valid also for three dimensional systems where the interval is replaced by volume, $\Delta x \rightarrow \Delta x \Delta y \Delta z$, as well as multidimensional systems of many particles.

The time dependent Schrödinger equation remains important for processes which are not stationary, it means when some change really happens. It is essential for our understanding of chemical reactions and matter changes as explained and applied in the following section.

Another feature of quantum formalism is the so called uncertainty relation. It follows from the properties of the wave equation, similar relations are known also in acoustics and applications of electric pulses: certain pairs of quantities are such that they can not be given both with infinite precision. In musical acoustics, the picking instruments with tones of short short duration have "uncertainty" in frequency. A clean frequency tone must last for a very long time, as for violins and wind instruments.

In addition to uncertainty of the discussed type, there are also two other features: any measurement process itself will require exchange of energy which can not be made negligible. Further, it will also change the wavefunction of the combined system consisting of the observed system and the observing device system. It means that any measurement result can be given only with a certain probability, it is not guaranteed that the measurement will happen. These features and the related phenomena of decoherence and entanglement make the quantum measurement fundamentally different from the understanding of it in classical physics. In Newtonian physics, measurement processes can be devised in such a way that energy and momentum exchange with the observed system are truly negligible, as for example observation of reflected light rays. In quantum physics the scattering of light can change the state of an atom or molecule.

2.2 Quantum mechanics and atomic level systems

Within the quantum perspective above supported by experiments, an atom is a structured object composed of a nucleus and electrons. The spectra and other features can be understood by studying the stationary states of the quantum models.

Orbitals in more complex objects, it means molecules and larger aggregates, are our mental mathematical images of where and how probable it is to detect an electron in a spatial region around that nuclei. Those orbitals shape the atomic and molecular structures, where each holds no more than two electrons which have furthermore opposite spins, a pure quantum phenomenon that has no classical analogue. Atoms interact with each other and aggregate in different molecular structures; free and chemically bonded atoms having an otherwise spherical electronic distribution can attract each other when they are a small distance apart. Such attraction, known as van der Waals, is electrostatic in origin, and is ascribed to either permanent-permanent, permanent-induced or instantaneous induced-induced dipoles interaction. However, when atoms approach each other too close, they repel each other due to the electrostatic repulsions of the like-charges, as well as Fermi repulsion, since each part of quantum space can be occupied by only one electron.

The effect of aggregation of atoms into complex structures can be described by studying the stationary states of electrons and nuclei of combined atomic subsystems. In the following we discuss how and why the nuclear and electronic motions can be considered separately. The n-electron wavefunctions in isolated atoms themselves or in combined structures as molecules, can in simplest cases be considered as wavefunctions for independent electrons. The effects of electron interactions and the Pauli principle are taken into account by so called self-consistent methods (as DFT or SCF bellow). Each of the electrons thus occupies

one spin orbital, which is the same as saying that two electrons with opposite spin can occupy one spatial orbital.

Atomic orbitals situated on different atoms will not generally remain valid single electron orbitals for the constructions mentioned above. New orbitals must be identified which best describe the electronic configurations in the fields of combined nuclei and the other electrons.

These new orbitals, or single electron states can be called molecular orbitals or Bloch states if the structures are periodic. For historical reasons there unfortunately exists a certain confusion in chemical literature, where two approximation assumptions about the molecular orbitals are presented as two distinct theories. From the point of physics, there is a need to define the hierarchy of approximations, where the famous Koster-Slater LCAO approach can serve as a basic approximation.

In this approach, the so called covalent bonding is a result of the fact that the energetically lowest stationary state in a situation with two (or in fact several) attraction centers is always lower than the lowest state created by any of the centers alone. As an example, the lowest state of one electron in the field of two protons situated at any distance will always be lower than the ground state of hydrogen. This fact is reflected by the existence of the H_2^+ molecular ion, the simplest system studied in molecular physics. The covalently bound molecule H_2 results when the two electrons are placed in the same spatial orbital. Bonding in systems where the participating electrons would originally belong to higher atomic orbitals follows the same principle, but becomes more complicated and leads to the geometrical features of molecules as discussed below.

In addition to the covalent bonding mentioned here there are also other types of electron rearrangements. The most important is probably the so called delocalized bonds important mainly in metals and in many carbon structures. Another one is the so called ionic bonding which is in fact the same as the covalent bonding, but the orbitals are highly localized on one of the centers. Due to this localization, the combined system appears as one negative and one positive ion. The fourth known bonding interaction is called hydrogen bonding. In Chemistry it is generally described by the attraction between the positive partial charge on a hydrogen covalently bonded to Oxygen, Nitrogen or Sulfur and the negative charge density of a lone-pair on another Oxygen, Nitrogen or Sulfur. That is the molecular orbital involves contributions from three atoms rather than just two [15] in such a way that the overall wavefunction is a linear combination of the wavefunction corresponding to the covalent bond and the wavefunction corresponding to the lone-pair. The hydrogen bond has somehow a directional character but it is weaker than the covalent bond, it is strongest when the three atoms are aligned where the hydrogen lies unequally in between.

The just mentioned mechanisms are important to explain the stability of our physical world and only quantum theory gives us parts of that explanation, where one should in principle solve the many particle molecular Schrödinger equation. Exact and analytical solutions for these wavefunctions are in practice impossible, therefore approximation schemes must be used.

To predict the dynamical evolution of a system of such small particles, one needs to solve the time dependent Schrödinger wave equation to be able to describe chemical reactions, condensation into solid state or melting of solid structures. A method to decouple, separate, the motion of electrons and nuclei called Born-Oppenheimer approach is in principle the basis of most of the applications of quantum theory to the analysis of chemical phenomena. In the following, this approach will be introduced. The presentation is to some degree based on ref. [5, 10] where also other references and details can be found.

2.2.1 Molecular structure: Separation of electronic and nuclear degrees of freedom

A molecular system with the positions of N nuclei, $R = \{R_1,\ R_2,\ \cdots,\ R_N\}$, and the n electrons located at $r = \{r_1,\ r_2,\ \cdots,\ r_n\}$, is completely described nonrelativistically by the molecular Schrödinger equation

$$\imath\hbar\frac{\partial}{\partial t}\ \Phi\left(r, R; t\right) = \mathcal{H}\ \Phi\left(r, R; t\right) \tag{2.9}$$

where $\mathcal{H}$ is the nonrelativistic molecular Hamiltonian, in SI units, of the N nuclei and n electrons, and it has the form

$$\begin{aligned}\mathcal{H}\left(R, r\right) \;=\; & -\sum_{I=1}^{N}\frac{\hbar^2}{2M_I}\nabla_{R_I}^2 - \sum_{\imath=1}^{n}\frac{\hbar^2}{2m_e}\nabla_{r_\imath}^2 \\ & + \sum_{\substack{I=1,\\ J>I}}^{N-1}\sum^{N}\frac{Z_I Z_J e^2}{4\pi\epsilon_0|R_J - R_I|} + \sum_{\substack{\imath=1,\\ \jmath>\imath}}^{n-1}\sum^{n}\frac{e^2}{4\pi\epsilon_0\ |r_\jmath - r_\imath|} + \sum_{\substack{I=1\\ \imath=1}}^{N}\sum^{n}\frac{Z_I e^2}{4\pi\epsilon_0|R_I - r_\imath|}\end{aligned} \tag{2.10}$$

the first term on the right-hand side of the above equation is the nuclear kinetic energy operator, the electronic kinetic energy operator is second, whereas the last three terms correspond respectively to the internuclear, inter-electronic and nuclear-electronic electrostatic interactions. M_I is the mass of nucleus I whose atomic number is Z_I, m_e is the mass of the electron, and e is its charge. The operators ∇_{R_I} and $\nabla_{r_\imath}$ act on the coordinates of nucleus I and electron $\imath$ respectively.

The electron-nucleus interactions bind electrons to nuclei, and leads to a mathematical inseparable Hamiltonian. Born and Oppenheimer based their method on the observation

that the motion of the nuclei must be much slower than the motion of electrons, mainly due to the big nucleus-electron mass ratio. Since energy according to the classical kinetic theory is equipartitioned over all degrees of freedom

$$m_e\omega_e^2 = M_I\omega_I^2 \rightarrow \frac{\omega_e}{\omega_I} \approx \sqrt{\frac{M_I}{m_e}} \approx 100. \tag{2.11}$$

A treatable method thus becomes to solve first the equations for the fast moving electrons for fixed configurations R of the nuclei, and only then allow the nuclear motion to be solved in the resulting field of already known electronic motion. This is equivalent to rewriting the molecular Hamiltonian as

$$\mathcal{H}(R,r) = T(R) + \mathcal{H}_e(R,r) \tag{2.12}$$

where the electronic Hamiltonian is

$$\mathcal{H}_e(R,r) = T(r) + V(R) + V(r) + V(R,r) = T(r) + V_t(r,R) \tag{2.13}$$

where $T(r)$, $V(R)$, $V(r)$, and $V(R,r)$ respectively represent: the electronic kinetic operator, nuclear-nuclear and electron-electron repulsion, and nuclear-electron attraction.
The stationary schödinger equation for the electronic Hamiltonian Eq.(2.13) is assumed solvable, moreover its solution is a set of orthonormal discrete eigenfunctions in the form, $\Psi_k(r,R)$, with a parametric dependence on the nuclear configuration $R \equiv R(t)$.

$$\mathcal{H}_e(r,R)\ \ \Psi_k(r,R) = E_k(R)\ \ \Psi_k(r,R) \tag{2.14}$$

Note that $\Psi_k(r,R)$ is multielectron wavefunction. The detailed determination of their form is usually done with the help of further approximations. The simplest forms are based on the so called Slater determinants which in turn are antisymmetrized versions of the independent electron approximation. Thus

$$\Psi_k(r,R) = \mathcal{A}\big(\varphi_1(r_1,t),\varphi_2(r_2,t),\cdots\varphi_n(r_n,t);\alpha(1),\alpha(2),\cdots,\alpha(n);\beta(1),\beta(2),\cdots,\beta(n)\big) \tag{2.15}$$

where $\{\varphi_i\}$ are the space orbitals, α and β are the spin orbitals and each takes the spin up and spin down states, and the operator $\mathcal{A}$ represents the antisymmetrization of the product. In the two electron case,

$$\Psi_k(r,R) = N\big(\varphi_1(r_1,t)\,\varphi_2(r_2,t) \pm \varphi_2(r_1)\,\varphi_1(r_2)\big)\big(\alpha(1)\beta(2) \mp \alpha(2)\beta(1)\big) \tag{2.16}$$

Details of single particle operators are consistently simplified in the nowadays most used density functional theory (DFT), where the sketched effects of multielectron description do not need to be considered explicitly.

The set $\{\Psi_k(r,R)\}$ is known as the adiabatic basis set, and E_k being the adiabatic energy eigenvalues. Since the eigenfunctions form a complete set, the total wavefunction Φ can

be expanded in these bases, and takes the following form known as the Born-oppenheimer ansatz

$$\Phi\left(r,R;t\right)=\sum_{l}\ \chi_{l}\left(R,t\right)\ \Psi_{l}\left(r,R\right) \tag{2.17}$$

Substitution for Φ, Eq.(2.17), in Eq.(2.9), multiplication form left by $\left\langle \Psi_{k}\left(r,R\right)\right|$, and integration over the electronic coordinates, gives the set of coupled equations

$$\left[T\left(R\right)+E_{k}\right]\chi_{k}+\sum_{l}\ C_{kl}\ \chi_{l}=i\hbar\frac{\partial}{\partial t}\chi_{k} \tag{2.18}$$

where C_{kl} is termed as the coupling operator, and is defined as

$$C_{kl}=\sum_{I}\frac{-\hbar^{2}}{M_{I}}\ \left(\left\langle \Psi_{k}\right|\nabla_{R_{I}}^{2}\left|\Psi_{l}\right\rangle +\left\langle \Psi_{k}\right|\nabla_{R_{I}}\left|\Psi_{l}\right\rangle \nabla_{R_{I}}\right) \tag{2.19}$$

The adiabatic approximation

The electronic hamiltonian $\mathcal{H}_{e}$ depends parametrically on the nuclear configuration R, and since R is slowly varying, one can use of adiabatic approximation. In this respect, different electronic quantum states are weakly coupled, i.e., all the non-adiabatic off-diagonal terms, $(C_{kl}\rightarrow 0\ ,\forall\ k\neq l)$, are disregarded. The following analysis explains when the adiabatic approximation can be used

$$\mathcal{H}|\psi_{l}\rangle=E_{l}|\psi_{l}\rangle \tag{2.20}$$

$$\begin{aligned}\nabla_{R_{I}}\left(\mathcal{H}|\psi_{l}\rangle\right) &= \nabla_{R_{I}}\mathcal{H}|\psi_{l}\rangle+\mathcal{H}\nabla_{R_{I}}|\psi_{l}\rangle &(2.21)\\ &= \nabla_{R_{I}}E_{l}|\psi_{l}\rangle+E_{l}\nabla_{R_{I}}|\psi_{l}\rangle &(2.22)\end{aligned}$$

multiplying the right hand sides of Eqs.(2.21 and 2.22) by $\langle\psi_{k}|$

$$\begin{aligned}\langle\psi_{k}|\nabla_{R_{I}}\mathcal{H}|\psi_{l}\rangle+\langle\psi_{k}|\mathcal{H}\nabla_{R_{I}}|\psi_{l}\rangle &= \langle\psi_{k}|\nabla_{R_{I}}E_{l}|\psi_{l}\rangle+\langle\psi_{k}|E_{l}\nabla_{R_{I}}|\psi_{l}\rangle\\ \langle\psi_{k}|\nabla_{R_{I}}\mathcal{H}|\psi_{l}\rangle+\langle\mathcal{H}\psi_{k}|\nabla_{R_{I}}|\psi_{l}\rangle &= \langle\psi_{k}|\nabla_{R_{I}}E_{l}|\psi_{l}\rangle+E_{l}\langle\psi_{k}|\nabla_{R_{I}}|\psi_{l}\rangle\\ \langle\psi_{k}|\nabla_{R_{I}}\mathcal{H}|\psi_{l}\rangle+E_{k}\langle\psi_{k}|\nabla_{R_{I}}|\psi_{l}\rangle &= \langle\psi_{k}|\nabla_{R_{I}}E_{l}|\psi_{l}\rangle+E_{l}\langle\psi_{k}|\nabla_{R_{I}}|\psi_{l}\rangle &(2.23)\end{aligned}$$

the first term on the right hand side vanishes, and further manipulation of Eq.(2.23) gives

$$\begin{aligned}\langle\psi_{k}|\nabla_{R_{I}}\mathcal{H}|\psi_{l}\rangle &= \left(E_{l}-E_{k}\right)\langle\psi_{k}|\nabla_{R_{I}}|\psi_{l}\rangle\\ \frac{\langle\psi_{k}|\nabla_{R_{I}}\mathcal{H}|\psi_{l}\rangle}{\left(E_{l}-E_{k}\right)} &= \langle\psi_{k}|\nabla_{R_{I}}|\psi_{l}\rangle &(2.24)\end{aligned}$$

that is, only when the energy difference $(E_{l}-E_{k})$ is everywhere big, one can use the adiabatic approximation. It can be easily shown that $\left(\sum_{I}\frac{\hbar^{2}}{M_{I}}\ \left\langle \Psi_{k}\right|\nabla_{R_{I}}\left|\Psi_{k}\right\rangle \nabla_{R_{I}}=0\right)$. Thus, only the diagonal terms are to be considered

$$C_{kk}=\sum_{I}\frac{-\hbar^{2}}{M_{I}}\ \left\langle \Psi_{k}\right|\nabla_{R_{I}}^{2}\left|\Psi_{k}\right\rangle \tag{2.25}$$

which represents the adiabatic correction of the eigenvalues E_k. The result is a set of decoupled equations of the nuclear eigenfunctions, and implies that the nuclear motion does not change the electronic quantum state during the time evolution, i.e., electrons are bound to the nuclei and respond instantaneously to the slow nuclear motion.

$$\left[T\left(R\right)+E_k\left(R\right)\right]\chi_k+C_{kk}\ \chi_k=i\hbar\frac{\partial}{\partial t}\chi_k \tag{2.26}$$

Consequently, the wave function Eq.(2.17) is reduced to a single term wavefunction being a direct product of the electronic and nuclear wavefunctions

$$\Phi\left(r,R;t\right)=\ \chi_k\left(R,t\right)\ \Psi_k\left(r,R\right) \tag{2.27}$$

Born-Oppenheimer approximation

Born-Oppenheimer approximation assumes only very small changes in the adiabatic electronic quantum state (wavefunction) when the configuration, R, of the massive nuclei is by little and slowly changed near the equilibrium. Mathematically, derivatives operate over approximately the same dimensions, i.e., $\nabla_{R_I}\psi_k$ is of the same order as $\nabla_{r_i}\psi_k\ \sim\ p_e\psi_k$, where p_e is the momentum of an electron. Hence

$$\frac{\hbar}{2M_I}\nabla_{R_I}^2\psi_k\sim\frac{p_e^2}{2M_I}=\frac{m_e}{M_I}E_e\sim10^{-4}E_e$$

where $E_e\ =\ E_k-V(R)$ is the electronic kinetic energy. That is, the dependence of the electronic state on, R, is so weak that both first and second derivatives of the electronic state with respect to the nuclear configuration, R, are negligibly small. Thus the diagonal coupling terms, C_{kk}, are also ignored, and the nuclear Schrödinger equation now takes the form

$$\left[T\left(R\right)+E_k\left(R\right)\right]\chi_k=i\hbar\frac{\partial}{\partial t}\chi_k \tag{2.28}$$

and describes nuclei as moving in an effective potential, E_k, modified by all electrons. The electronic degrees of freedom no longer appear in the above equation since all electronic effects are now superimposed upon the slowly moving nuclei via the E_k term which is referred to as the "interatomic" potential energy surface.

Classical approximation of motion of nuclei in the adiabatic electronic basis

In the areas of atomic collisions and classical Molecular Dynamics, Chap.(3), nuclei are classical point particles moving according to Newton laws under the influence of their interatomic potential. To impose the classical point particle approximation on Eq.(2.28), the nuclear wavefunction corresponding to the k-electronic state is rewritten as

$$\chi_k\left(R;t\right)=A_k\left(R;t\right)\ \exp\left[\frac{\imath S_k\left(R;t\right)}{\hbar}\right] \tag{2.29}$$

with an amplitude A_k, and a phase factor S_k being both real. When Eq.(2.29) is substituted in Eq.(2.28), one obtains

$$\frac{\partial S_k}{\partial t} = -\sum_I \frac{(\nabla_{R_I} S_k)^2}{2M_I} - \sum_I \frac{\hbar^2}{2M_I}\frac{(\nabla^2_{R_I} A_k)}{A_k} \tag{2.30}$$

$$\frac{\partial A_k}{\partial t} = -\sum_I \frac{(\nabla_{R_I} A_k)(\nabla_{R_I} S_k)}{M_I} - \sum_I \frac{A_k(\nabla^2_{R_I} S_k)}{2M_I} \tag{2.31}$$

multiplying Eq.(2.31) from left by $2A_k$, gives

$$\frac{\partial {A^2}_k}{\partial t} = -\sum_I \frac{\nabla_{R_I}({A^2}_k \nabla_{R_I} S_k)}{M_I} \tag{2.32}$$

which is identified as the continuity equation for the probability density, $P = {A^2}_k$, and the current density, $J_I = \dfrac{{A^2}_k \nabla_I S_k}{M_I}$, in the k-electronic state. In the classical limit $\hbar \to 0$, then Eq.(2.30) becomes

$$\frac{\partial S_k}{\partial t} = -\sum_I \frac{(\nabla_{R_I} S_k)^2}{2M_I} - E_k \tag{2.33}$$

The nuclear velocity is given by

$$\dot{R}_I = \frac{J_I}{P} = \frac{\nabla_{R_I} S_k}{M_I} \tag{2.34}$$

the classical kinetic energy of nuclei evaluates to $T_k = \sum_I \dfrac{1}{2} M_I \dot{R}_I^2$, then Eq.(2.33) becomes

$$\frac{\partial S_k}{\partial t} = -(T_k + E_k) = -E_{\text{tot}} = \text{constant} \tag{2.35}$$

where E_{tot} is the constant total energy. Finally, applying the gradient on Eqs.(2.35) gives the classical "Newtonian" equations of motion for all nuclei in the k-electronic state

$$M_I \ddot{R}_I = -\nabla_{R_I} E_k \tag{2.36}$$

Considering only the electronic ground state wavefunction Ψ_0 of $\mathcal{H}_e$, defines the so-called ground state Born-oppenheimer potential energy surface

$$E_0^{\text{BO}} = \min_{\Psi_0} \left\{ \left\langle \Psi_0 \, | \mathcal{H}_e | \Psi_0 \right\rangle \right\} \tag{2.37}$$

2.3 Basic classical statistical Mechanics

Statistical mechanics is the field of physics which describes the phenomenological thermodynamics in relations to the classical microscopic behavior of atoms in the system in

question. That is, a macroscopic state (macrostate) described by thermodynamic quantities (experimental observables such as temperature and pressure, etc.), is statistically interpreted in terms of all the accessible microscopic mechanical states (microstates) where each is characterized by all the N atoms' positions, $\big(q_1, q_2, \cdots, q_N \equiv q^N\big)$, and momenta, $\big(p_1, p_2, \cdots, p_N \equiv p^N\big)$, i.e., points in the multidimensional phase space Γ. In a thermodynamic equilibrium, measurements of observables are invariant independently of the time of the measurements and the system's initial microstate. Theoretically and assuming that the equations of motion of the system are solved, each observable can be empirically associated with a function, $(\mathcal{O})$, of the instantaneous microstate, $\big(q^N(t), p^N(t)\big)$, of the system. The quantity $\mathcal{O}\big(q^N(t), p^N(t)\big)$ is not an observable since measurements are performed in a macroscopic time; thus any microscopic observable is assumed to be a time averaged value:s

$$\langle \mathcal{O} \rangle_t = \lim_{\tau \to \infty} \frac{1}{\tau} \int_{\tau_0}^{\tau_0 + \tau} \mathcal{O}\big(q^N(t), p^N(t)\big) dt \tag{2.38}$$

Thermodynamic observable can be alternatively modeled by considering at once a collection of identical systems. Each system represent one of all the accessible microstates, i.e all points in the phase space. If this collection (statistical ensemble) is allowed to evolve in time, its behavior can be characterized by a time dependent distribution function, $\rho\big(q^N(t), p^N(t)\big)$, for the microstates, i.e., the quantity $\displaystyle\int_{\mathcal{V}} \rho\Big(\big(q^N(t), p^N(t)\big)\Big)\ dq^N\ dp^N$ would give the average number of microstates in the region, $\mathcal{V}$, in the phase space. Obviously if we integrate over the whole volume in phase space, then $\displaystyle\int_{\Gamma} \rho\Big(\big(q^N(t), p^N(t)\big)\Big)\ dq^N\ dp^N = \mathcal{M}$, where $\mathcal{M}$ is the number of all accessible points in the phase space. The instantaneous average value of the observable, $\mathcal{O}$, over the phase space is now interpreted as

$$\frac{\int_{\Gamma} \mathcal{O}\big(q^N(t), p^N(t)\big) \rho\Big(\big(q^N(t), p^N(t)\big)\Big)\ dq^N\ dp^N}{\int_{\Gamma} \rho\Big(\big(q^N(t), p^N(t)\big)\Big)\ dq^N\ dp^N} \tag{2.39}$$

If we assume equal probability for all microstates, then the distribution of points in phase space is frozen into one single shape, i.e., the distribution function is time invariant, and the condition

$$\frac{d\rho\big(q^N(t), p^N(t)\big)}{dt} = 0 \tag{2.40}$$

describes the thermodynamic equilibrium. The the so-called ensemble average is defined as

$$\langle \mathcal{O} \rangle_{ensemble} = \frac{\int_{\Gamma} \mathcal{O}\big(q^N, p^N\big) \rho\Big(\big(q^N, p^N\big)\Big)\ dq^N\ dp^N}{\int_{\Gamma} \rho\Big(\big(q^N, p^N\big)\Big)\ dq^N\ dp^N} \tag{2.41}$$

The ergodic hypothesis states that in thermodynamic equilibrium, the time average and the ensemble average are equal. That is, if one allows the system to evolve indefinitely in

time, the system will pass through all possible microstates, and the experimental measurement will coincide with the calculated time and ensemble averages. Liouville's theorem asserts the relation Eq.(2.40), when the Hamiltonian is conserved, that is the distribution function is constant along any trajectory in the phase space. Liouville's theorem ensures thus, independently from ergodic hypothesis, the equality between time averages and their corresponding ensemble averages.

Statistical ensembles

The three most popular statistical ensembles in classical molecular dynamics simulations are mentioned below:

The microcanonical ensemble is the thermodynamic state defined by a fixed number of atoms,N , constant volume, V, and energy, E. It corresponds to an isolated system and sometimes known denoted as NVE ensemble.

The canonical (NVT) ensemble is a collection of all systems whose thermodynamic state is characterized by a fixed number of atoms, N,,a constant volume, V, and temperature, T.

The Isobaric-Isothermal (NPT) ensemble is the state where the number of atoms, N, pressure, P, and temperature, T, are all constants.

The distribution function of an ensemble has the following form

$$\rho(q^N, p^N) \sim \exp\left(\frac{-\mathcal{H}(q^N, p^N)}{K_B T}\right)$$

and the distribution density can be defined as

$$\frac{\rho(q^N, p^N)}{Z}$$

where $\mathcal{H}$ is the classical Hamiltonian, T is the temperature, k_B is Boltzmann's constant and Z, the normalization constant, is known as the partition function defined as

$$Z = \int dq^N dp^N \rho(q^N, p^N)$$

It is of a usual difficulty to solve Eq.(2.41) since all the accessible microstates must be previously known. However, in classical molecular dynamics points in an ensemble are calculated sequentially over a long time, and one can the compute the time average

$$\langle \mathcal{O} \rangle_t \approx \frac{1}{n} \sum_{t=1}^{n} \mathcal{O}\big(q^N(t), p^N(t)\big) \tag{2.42}$$

where t is time, n is the number of timesteps or the number of times calculations were performed, and $\mathcal{O}\big(p^N(t), r^N(t)\big)$ is clearly the instantaneous value of the $\mathcal{O}$-observable.

Time Averages in Molecular Dynamics

Time average of the potential energy

$$\langle V \rangle = \frac{1}{n} \sum_{t=1}^{n} \left(\sum_{i=1}^{N} V(q_i(t), p_i(t)) \right) \tag{2.43}$$

where the index i marks atoms, and V is written here as a function of positions and momenta for a generality, even though it is in most cases velocity-independent.
Time average of the kinetic energy

$$\langle E_k \rangle = \frac{1}{n} \sum_{t=1}^{n} \left(\sum_{i=1}^{N} \frac{p_i(t)^2}{2m_i} \right) \tag{2.44}$$

where m_i is the mass of the particle i, and p_i is its momentum. Remember that, to rely on the values computed above, the molecular dynamics simulation must run for a sufficiently long time so that enough representative configuration are sampled i.e. the system will have traveled through enough points in the phase space.

Chapter 3

Molecular Dynamics

Molecular dynamics (MD) is a specialized computer-based discipline to simulate time evolving atomistic or molecular systems. In such simulations, motion of atoms is determined within the framework of classical mechanics, this is carried out in intention to reveal the structural and energetics information. The extracted information of the so many microscopic dynamical states, over a certain period, are condensed and employed by means of statistical mechanics to calculate macroscopic and bulk properties of solids, liquids as well as gases. Yet MD is a powerful computational approach, and is mainly used to compute macroscopic properties that include structures, thermodynamics e.g. enthalpy, temperature and pressure, and transport properties e.g. thermal conductivity, viscosity and diffusion.
In a molecular system, each atom is subjected to intermolecular forces derived from a single pre-defined potential energy surface set up by the rest of the system constituents, electrons as well as nuclei, yet motion of a single atom influences all the others, coupling thus their Newtonian equations of motion. To analytically solve (integrate) the aforesaid coupled Newtonian second order differential equations for a vast number, thousands to millions, of particles is out of reach; numerical methods, using the so-called time integration algorithm Sec.(3.1.2), are thus implemented to overcome this problem and compute the classical trajectories of atoms in the system.

Molecular dynamics is an in-between-theory-and-experiment discipline, and it is used to either investigate and verify a theoretical model describing physical and chemical processes, or perform a very low-cost virtual experiment on a computer screen. Given a theoretical model with varying complexity, calculations are carried out using a computer algorithm, results are then compared with experimental measurements and/or first principles' calculations. MD provides thus a possibility to modify the model in a hand, or research and study some experimentally-inaccessible phenomena if the model is validated.

Molecular systems and motion of their constituents, both nuclei and electrons, are known

to be accurately described only by laws of quantum mechanics; why is it then Newtonian mechanics used to describe that motion of atoms (nuclei) in molecular dynamics?
Well, implementation of classical laws of mechanics in this scheme involves a series of approximations for the quantum description; first, the molecular wavefunction (solution) of the molecular Schrödinger equation is separated into nuclear and electronic parts according to Born-Oppenheimer approximation, Sec.(2.2.1), so that motion of nuclei is decoupled from electronic motion due to the fact that nuclei are much heavier. Such decoupling allows their equations of motion to be separated and solved. Second, nuclei are approximated as classical particles, Sec.(3.1.1) and Sec.(2.2.1). Third, electronic variables are either integrated out beforehand and an approximate single potential energy surface (usually representing the electronic ground state) is constructed, or they are treated within a suitable approximation as active degrees of freedom via the electronic schrödinger equation, and forces on nuclei are computed by electronic structure calculations that are performed for each generated trajectory. Accordingly, MD simulation is branched out into two methodologies:

1. Classical Molecular Dynamics, Sec.(3.1), where forces are derived from predefined potential models by analytical gradient applications.

2. *Ab initio* Molecular Dynamics, Sec.(3.2), where forces on nuclei are obtained from the electronic structure calculations.

Herein and in the next chapter, we would briefly introduce and describe the basics and basic machineries of molecular dynamics, see Refs.([2, 12, 23, 27, 28, 33, 39]) for further in-depth and detailed discussions and analysis. For concerns in first principle molecular dynamics for excited states and nonadiabatic transition , see Refs([10, 22]).

3.1 Classical Molecular Dynamics

Classical molecular dynamics requires a predefined potential energy function representing Born-Oppenheimer ground state potential surface. This function, and based on scientific intuitions, is empirically constructed and fitted to experimental observations, yet casted in a functional form of geometrical quantities, e.g., relative distances, angles. Interatomic potentials effectively sum up all the inter- and intramolecular electrostatic interactions. Time variation of the electric and magnetic fields due to motion of charges are (assumed) small and spin interactions are ignored, therefore magnetic effects are dropped out. The interatomic (electrostatic) forces are conservative, since the electric field in a molecule is irrotational by assumption. That is, forces depend only on positions and has no explicit time dependence, thus they can be represented by a position-dependent potential energy

function satisfying the following

$$F_I = M_I \ddot{R}_I = -\frac{\partial}{\partial \vec{R}_I} V(\vec{R}_1,\ \vec{R}_2,\ ...,\ \vec{R}_N), \quad I = 1,\ 2,\ ...,\ N \tag{3.1}$$

where $F_I,\ M_I,\ R_I$ are the respective force, mass and position of $I-$th atom , and V is the potential function that depends on all atomic positions and thereby, couples the 'classically interpreted' motion of atoms. If the interacting particles in the simulation are molecules rather than atoms, then also the equations of the rotational motion must be integrated since neither sizes molecules nor their spherical asymmetry can be neglected anymore.

3.1.1 Derivation of Classical Molecular Dynamics

Following references [27, 28], we show how to understand the classical molecular dynamics from the quantum point of view. Considering once more the molecular non-relativistic time-dependent schödinger equation Eq.(2.9), with $\Phi(r, R; t)$ being the total wavefunction of electronic, nuclear degrees of freedom and time, and $\mathcal{H}$ is the Hamiltonian given by Eq.(2.10).
Invoking the time dependent self consistent field approximation (TDSCF), i.e, a separable total wavefunction is written as a single determinant (configuration) ansatz

$$\Phi(r, R; t) \approx \Psi(r; t)\ \chi(R; t)\ \exp\left[\frac{\imath}{\hbar}\int_{t_0}^{t} dt' E_e(t')\right] \tag{3.2}$$

where the electronic and nuclear wavefunctions are separately normalized

$$\langle \Psi(r; t) | \Psi(r; t) \rangle = 1, \qquad \langle \chi(R; t) | \chi(R; t) \rangle = 1$$

and the phase factor has the form

$$E_e = \int dr dR\ \Psi^{\star}(r; t)\ \chi^{\star}(R; t)\ \mathcal{H}_e\ \Psi(r; t)\ \chi(R; t) \tag{3.3}$$

Inserting Eq.(3.2) into the molecular schrödinger Eq.(2.9), with $\mathcal{H}$ being defined in Eq.(2.12) and Eq.(2.13), multiply from left by $\langle \Psi(r; t) |$ and $\langle \chi(R; t) |$, integrate over R and r, and apply the energy conservation

$$\frac{d}{dt} \int \Phi^{\star}(r, R; t)\ \mathcal{H}\ \Phi(r, R; t)\ = 0$$

the following system of coupled equations is obtained

$$\begin{aligned} \imath\hbar\frac{\partial\Psi}{\partial t} &= -\sum_i \frac{\hbar^2}{2m_e}\nabla^2_{r_i}\Psi + \\ &\quad \left\{\int drdR\ \chi^\star(R;t)\ V_t(r,R)\ \chi(R;t)\right\}\Psi \qquad (3.4) \\ \imath\hbar\frac{\partial\chi}{\partial t} &= -\sum_I \frac{\hbar^2}{2M_I}\nabla^2_{R_I}\chi + \\ &\quad \left\{\int drdR\ \Psi^\star(r;t)\ \mathcal{H}_e(r,R)\ \Psi(r;t)\right\}\chi \qquad (3.5) \end{aligned}$$

which defines the basis of the TDSCF. Each wavefunction above obey Schödinger equation but with time dependent effective potential obtained by appropriate averages over the other degrees of freedom; the quantum mechanical expectation values of the coulombic electrons-nuclei attractions for the electronic wavefunction, and the electronic hamiltonian for the nuclear wavefunctions. These averages and the ansatz Eq.(3.2) lead to a mean-field description of the coupled dynamics of electrons and nuclei.
Imposing the classical point particle representation (approximation) for nuclei, their corresponding wavefunction is rewritten as

$$\chi(R;t) = A(R;t)\ \exp\left[\frac{\imath S(R;t)}{\hbar}\right] \qquad (3.6)$$

the amplitude $A > 0$ and the phase factor S are both real. Substitution in Eq.(3.5) for the nuclei in TDSCF system, and then separating of the real and imaginary parts reads as

$$\frac{\partial S}{\partial t} + \sum_I \frac{1}{2M_I}(\nabla_{R_I}S)^2 + \int dr\Psi^\star\mathcal{H}_e\Psi = \hbar^2\ \sum_I\ \frac{1}{2M_I}\frac{(\nabla^2_{R_I}A)}{A} \qquad (3.7)$$

$$\frac{\partial A}{\partial t} + \sum_I \frac{1}{M_I}(\nabla_{R_I}A)(\nabla_{R_I}S) + \sum_I \frac{1}{2M_I}A(\nabla^2_{R_I}S) = 0 \qquad (3.8)$$

Eqs.(3.7,3.8) in the new variables A and S correspond exactly to Eq.(3.5). More important, the term containing $\hbar$ in Eq.(3.7) vanishes at the classical limit, and Eq(3.7) is reduced to:

$$\frac{\partial S}{\partial t} + \sum_I \frac{1}{2M_I}(\nabla_{R_I}S)^2 + \int dr\Psi^\star\mathcal{H}_e\Psi = 0 \qquad (3.9)$$

which is similar to Hamiltonian-Jacobi equations of motions:

$$\frac{\partial S}{\partial t} + H(R, \nabla_I S) = 0 \qquad (3.10)$$

with H being the classical hamiltonian:

$$H(R,P) = T(P) + V(R) \qquad (3.11)$$

where R and P are respectively the generalized coordinates and their conjugate momenta, and relate one another by the following transformation

$$P_I \equiv \nabla_{R_I} S\left(R\left(t\right);t\right)$$

Newtonian equations of motion for nuclei $\dot{P}_I = -\nabla_{R_I} V\left(R\right)$ corresponding to Eq.(3.9) are then

$$\dot{P}_I = M_I \ddot{R}_I\left(t\right) = -\nabla_{R_I} \int dr\ \Psi^{\star} \mathcal{H}_e \Psi = -\nabla_{R_I} V_e^{\mathrm{Ehr}}\left(R\left(t\right)\right) \tag{3.12}$$

that is, nuclei move now according to laws of classical mechanics in the effective potential set up by all electrons. This potential depends only on the nuclear positions at a time t, and is the electronic hamiltonian, $\mathcal{H}_e$, averaged over electronic degrees of freedom when the instantaneous set of nuclear positions $R\left(t\right)$ is kept fixed. However, the nuclear wavefunction $\chi\left(R_I;t\right)$ appears in the electronic part Eq.(3.4), it has to be replaced by the nuclear positions for consistency; this is achieved by replacing the nuclear probability density $\left|\chi\left(R;t\right)\right|^2$ by a delta-functions product $\prod_I \delta\left(R_I - R_I\left(t\right)\right)$ centered at the classical nuclear instantaneous positions R_I given by Eq.(3.12), the expectation values of nuclear positions are thus

$$\int dR\ \chi^{\star}\left(R;t\right)\ R_I\ \chi\left(R;t\right) \overset{\hbar\to 0}{\longrightarrow} R_I\left(t\right) \tag{3.13}$$

at this classical limit, the electronic time dependent schrödinger 'wave' equation is

$$\begin{aligned} \imath\hbar\frac{\partial\Psi}{\partial t} &= -\sum_i \frac{\hbar^2}{2m_e}\nabla_{r_i}^2\Psi + V_t\left(r,R\left(t\right)\right)\ \Psi \\ &= \mathcal{H}_e\left(r,R\left(t\right)\right)\ \Psi\left(r,R;t\right) \end{aligned} \tag{3.14}$$

which shows that electrons evolve quantum mechanically and self-consistently with the classically moving nuclei according to Eq.(3.12). Now $\mathcal{H}_e$, therefore Ψ, depends parametrically on the classical nuclear positions $\{R\left(t\right)\}$ at time "t" through the potential $V_t\left(r,R\left(t\right)\right)$. Up to the present stage, only nuclei behave like classical particles, whereas electrons are still quantum objects. Moreover, transition between different electronic states is possible though the TDSCF leads to a mean field theory. This can be realized if the electronic wavefunction Ψ for a fixed time "t" is expanded in an appropriate basis of many electronic states or determinants Ψ_k

$$\Psi\left(r,R;t\right) = \sum_{k=0}^{\infty} c_k\left(t\right)\ \Psi_k\left(r;R\right) \tag{3.15}$$

the $c_k\left(t\right)$ coefficients are complex, with the properties $\sum_k \left|c_k\left(t\right)\right|^2 \equiv 1$, and $\left|c_k t\right|^2$ explicitly describe the time evolution of the occupancy of the different k-states. One choice of the basis set is the "instantaneous" orthonormal adiabatic basis functions $\{\Psi_k\}$ which result from solving the time-independent schrödinger equation

$$\mathcal{H}_e\left(r;R\left(t\right)\right)\ \Psi_k\left(r;R\left(t\right)\right) = E_k\left(R\left(t\right)\right)\ \Psi_k\left(r;R\left(t\right)\right) \tag{3.16}$$

where the instantaneous nuclear positions $\{R(t)\}$ at a time "t", is substituted from Eq.(3.12), $\{E_k\}$ is the set of energy eigenvalues corresponding to the electronic hamiltonian $\mathcal{H}_e$, and $\{\Psi_k\}$ are their associated eigenfunctions.
To examine the possible transition between different electronic states, we insert the electronic wave function expansion, Eq.(3.15), within the adiabatic basis obtained from Eq.(3.16), into the force equation of the classical nuclei, Eq.(3.12), Hellmann-Feynman theorem then yields

$$F_I = M_I \ddot{R}_I(t) = -\langle \Psi | \nabla_{R_I} \mathcal{H}_e | \Psi \rangle \tag{3.17}$$

$$\begin{aligned}
\nabla_{R_I} \langle \Psi | \mathcal{H}_e | \Psi \rangle &= \sum_{k,l} c_k^\star(t)\, c_l(t)\ \nabla_{R_I} \Big\langle \Psi_k | \mathcal{H}_e | \Psi_l \Big\rangle = \sum_k c_k^\star(t)\ \sum_l c_l(t)\ \nabla_{R_I} E_l\ \delta_{kl} \\
&= \sum_{k,l} c_k^\star(t)\, c_l(t) \left(\Big\langle \nabla_{R_I} \Psi_k | \mathcal{H}_e | \Psi_l \Big\rangle + \Big\langle \Psi_k | \mathcal{H}_e | \nabla_{R_I} \Psi_l \Big\rangle + \Big\langle \Psi_k | \nabla_{R_I} \mathcal{H}_e | \Psi_l \Big\rangle \right) \\
&= \sum_{k,l} c_k^\star(t)\, c_l(t) \left(E_l \Big\langle \nabla_{R_I} \Psi_k | \Psi_l \Big\rangle + E_k \Big\langle \Psi_k | \nabla_{R_I} \Psi_l \Big\rangle + \Big\langle \Psi_k | \nabla_{R_I} \mathcal{H}_e | \Psi_l \Big\rangle \right)
\end{aligned} \tag{3.18}$$

because the electronic eigenfunctions are orthonormalized

$$\begin{aligned}
\delta_{kl} &= \Big\langle \Psi_k | \Psi_l \Big\rangle \\
0 &= \nabla_I \Big\langle \Psi_k | \Psi_l \Big\rangle = \Big\langle \nabla_{R_I} \Psi_k | \Psi_l \Big\rangle + \Big\langle \Psi_k | \nabla_{R_I} \Psi_l \Big\rangle \rightarrow \Big\langle \nabla_{R_I} \Psi_k | \Psi_l \Big\rangle = -\Big\langle \Psi_k | \nabla_{R_I} \Psi_l \Big\rangle
\end{aligned}$$

then, Eq.(3.18) with a little rearrangement becomes

$$\begin{aligned}
-\langle \Psi | \nabla_{R_I} \mathcal{H}_e | \Psi \rangle &= \sum_{k,l} c_k^\star(t)\, c_l(t)\ \left(-\nabla_{R_I} E_l\ \delta_{kl} + E_l \Big\langle \nabla_{R_I} \Psi_k | \Psi_l \Big\rangle + E_k \Big\langle \Psi_k | \nabla_{R_I} \Psi_l \Big\rangle \right) \\
&= -\sum_k |c_k(t)|^2\, \nabla_{R_I} E_k + \sum_{k,l} c_k^\star(t)\, c_l(t)\, (E_k - E_l) \Big\langle \Psi_k | \nabla_{R_I} \Psi_l \Big\rangle
\end{aligned}$$

but the hermitianity of the electronic hamiltonian gives

$$\begin{aligned}
\Big\langle \Psi_l | \mathcal{H} | \nabla_{R_I} \Psi_k \Big\rangle = \Big\langle \Psi_l E_l | \nabla_{R_I} \Psi_k \Big\rangle &= \Big\langle \nabla_{R_I} \Psi_k | \mathcal{H} | \Psi_l \Big\rangle^\star \\
&= \Big\langle \nabla_{R_I} \Psi_k | E_k \Psi_l \Big\rangle^\star = \Big\langle \Psi_l E_k | \nabla_{R_I} \Psi_k \Big\rangle
\end{aligned}$$

and the equations of motion of nuclei in the adiabatic basis are thus given by

$$M_I \ddot{R}_I(t) = -\sum_k |c_k(t)|^2\, \nabla_{R_I} E_k - \sum_{k,l} c_k^\star(t)\, c_l(t)\, (E_k - E_l)\, d_I^{kl} \tag{3.19}$$

where

$$d_I^{kl}(R(t)) = \Big\langle \Psi_k\ | \nabla_{R_I} \Psi_l \Big\rangle; \quad d_I^{kk}(R(t)) \equiv \Big\langle \Psi_k\ | \nabla_{R_I} \Psi_k \Big\rangle = 0 \tag{3.20}$$

are the non-adiabatic coupling terms. To evaluate the time evolution of the time-dependent expansion coefficients of the time-dependent electronic wavefunction in the adiabatic basis from Eq.(3.16), ,substitute Eq.(3.15) into the time dependent electronic schrödinger equation Eq.(3.14) is

$$\begin{aligned}\mathcal{H}_e \sum_l c_l(t) \left|\Psi_l\right\rangle &= \imath\hbar \frac{\partial}{\partial t} \sum_l c_l(t) \left|\Psi_l\right\rangle \\ &= \imath\hbar \sum_l \dot{c}_l(t) \left|\Psi_l\right\rangle + \imath\hbar \sum_l c_l(t) \frac{\partial}{\partial t} \left|\Psi_l\right\rangle \\ &= \imath\hbar \sum_l \dot{c}_l(t) \left|\Psi_l\right\rangle + \imath\hbar \sum_l \sum_I c_l(t) \nabla_{R_I} \left|\Psi_l\right\rangle \frac{\partial R_I}{\partial t} \end{aligned} \tag{3.21}$$

where

$$\frac{\partial}{\partial t}\Psi_l = \sum_I \nabla_{R_I} \Psi_l \frac{\partial R_I}{\partial t}$$

multiplying both sides of Eq.(3.21) from left by $\left\langle \Psi_k \right|$, gives

$$c_k(t) E_k = \imath\hbar \dot{c}_k(t) + \imath\hbar \sum_{I,l} c_l(t) \dot{R}_I d_I^{kl} \tag{3.22}$$

which shows the possible non-adiabatic transition between the electronic states Ψ_k and Ψ_l, where $|c_k(t)|^2$ is now interpreted as the probability density of finding the system is in the adiabatic state Ψ_k at time "t".

When the energy difference between the ground and the first excited states is everywhere large in comparison with the thermal energy, the electronic wave function at each time instant can be restricted to the ground state Ψ_0 of the electronic hamiltonian $\mathcal{H}_e$ in Eq.(3.16), i.e., $|c_0(t)|^2 = 1$ in Eq.(3.16). In such a limit, the nuclei move on the single potential energy surface defined by

$$V_e^{\text{Ehr}} = \left\langle \Psi_0 \left| \mathcal{H}_e \right| \Psi_0 \right\rangle \equiv E_0(R) \tag{3.23}$$

which is computed by solving the electronic time-independent schrödinger equation only for the ground state:

$$\mathcal{H}_e \Psi_0 = E_0 \Psi_0 \tag{3.24}$$

Now, E_0 is a function of nuclear positions R, and both Ehrenfest- and the ground state Born-Oppenheimer potentials are identical.

Furthermore the overall "internal interaction" potential is approximated to V^{appr} which is expanded to pair-wise, three-body, four-body and up to n-body contributions, these contributions are categorized as intermolecular long-range and intramolecular short-range

interactions

$$V^{\text{Ehr}} \approx V^{\text{appr}}(R) = \sum_{I<J}^{N} V_{IJ}(R_I, R_J) + \sum_{I<J<K}^{N} V_{IJK}(R_I, R_J, R_K) + \sum_{I<J<K<L}^{N} V_{IJKL}(R_I, R_J, R_K, R_L) + \cdots \quad (3.25)$$

Potential expansion is practically truncated at some term to reduce the dimensionality resulting from the increase of the number of active nuclear degrees of freedom. Within the same potential expansion, electronic degrees of freedom do no longer appear explicitly but are effectively included in a functional form of V^{appr} potential.

Equation (3.23) justifies the separation of computations of nuclear dynamics from that of the potential energy hypersurface. Assuming the possibility to solve the stationary scrödinger equation (3.16) for as many nuclear configurations as possible, the classical molecular dynamics approach is derived by the following three step scheme:

1. Solving Eq.(3.24) for many representative nuclear configurations to compute the ground state energy E_0.
2. The generated data points $\left(R, V^{\text{Ehr}}(R)\right)$ or some equivalent experimental data points are fitted to a suitable analytical functional form to construct a global potential energy surface.
3. The following Newtonian equation of motion

   $$M_I \ddot{R}_I(t) = -\nabla_{R_I} V^{\text{appr}} \quad (3.26)$$

   is solved by applying analytically the gradient for many different initial conditions to produce the nuclear classical trajectories on this global potential energy surface.

Classical Molecular Dynamics, revisited

In classical molecular dynamics, the quantum electrons are assumed to remain in their instantaneous eigenstate (no change in their configurations) as they only respond instantaneously to the much slower motion of nuclei, henceforth their degrees of freedom are integrated out. Thereafter nuclei evolve classically on one single Born-Oppenheimer potential energy surface represented by a functional form which effectively includes the electronic effects. The single Born-Oppenheimer potential energy surface is traditionally identified by the electronic ground state. It is now an entire classical mechanical problem, quantum mechanical effects were by construction excluded, and so are chemical reactions, bond formation or breaking, i.e., chemistry is hardly understood in such scheme.

3.1.2 Finite difference method and the integration algorithm

Finite difference method:

Exact analytical formulae of solutions to initial value problems are usually rare and generally difficult to find, they are furthermore not suitable to implement on computers. An alternative method is to find an approximate function, or its discrete approximation, which satisfies the differential equations along with their initial (boundary) conditions. One approach is to provide numerical approximate solutions to differential equation problems based on the finite difference approach. In this method, the differential equation is transformed into a finite difference problem by discretizing the domain, continuous independent variable(s) of the solution function, into infinitesimally separated points on a grid, the separation between any two adjacent points is known as the step. The discrete approximate solutions are found at the grid's successive points only and count for the overall solution. The finite difference formulas are continuous obtained from Taylor expansion truncated at some term, derivatives in the differential equation are then replaced by finite difference approximations based only on values of the function itself at those discrete points.

Finite difference approximation for derivatives of a univariate function

From calculus, a derivative of a univariate function is defined as

$$\frac{df}{dx} \equiv f'(x) := \lim_{\delta x \to 0} \frac{f(x+\delta x) - f(x)}{\delta x}$$

omitting the limit in the above expression is a valid approximation as long as the δx is finite and small, if the continuous independent variable x is further discretized on a grid such that $x_{n+1} = x_n + \delta x$, then

$$\left[\frac{df}{dx}\right]_n^+ := \frac{f(x_{n+1}) - f(x_n)}{\delta x} \tag{3.27}$$

where n indicates the grid point at which the derivative is approximated, and $+$ sign indicates the so-called forward approximation. Considering a third-order taylor expansion of $f(x)$ at the point x_{n+1} reads:

$$f(x_{n+1}) = f(x_n) + \delta x f'(x_n) + \frac{1}{2}\, f''(x_n)\delta x^2 + \frac{1}{6}\, f'''(x_n)\delta x^3 + O(\delta x^4) \tag{3.28}$$

A backward approximation is also possible and it takes the form:

$$\left[\frac{df}{dx}\right]_n^- := \frac{f(x_n) - f(x_{n-1})}{\delta x} \tag{3.29}$$

where the third-order taylor expansion at the point $x_{n-1} = x_n - \delta x$ is:

$$f(x_{n-1}) = f(x_n) - \delta x f'(x_n) + \frac{1}{2}\, f''(x_n)\delta x^2 - \frac{1}{6}\, f'''(x_n)\delta x^3 + O(\delta x^4) \tag{3.30}$$

each of the above one-sided (forward and backward) approximations to the first derivative has a first order accuracy, i.e., the discretization (truncation) error is of the order $O(\delta x)$. An alternative approximation, simply the average of the two one-sided above, is referred to as the centered approximation, and is expressed:

$$\left[\frac{df}{dx}\right]_n^0 := \frac{f(x_{n+1}) - f(x_{n-1})}{2\delta x} = \frac{1}{2}\left(\left[\frac{df}{dx}\right]_n^+ + \left[\frac{df}{dx}\right]_n^- \right) \tag{3.31}$$

substituting *eq(3.28)* and *eq(3.30)* into *eq(3.31)*, the centered approximation reads:

$$\left[\frac{df}{dx}\right]_n^0 = f'(x_n) + O(\delta x^2)$$

which clearly exhibits a second order accuracy.

The finite difference approximation for a second order derivative can be computed in analogous ways, the forward approximation is:

$$\begin{aligned}
\left[\frac{d^2f}{dx^2}\right]_n^+ &:= \frac{f'(x_{n+1}) - f'(x_n)}{\delta x} \\
&= \frac{1}{\delta x}\left[\left(\frac{f(x_{n+2}) - f(x_{n+1})}{\delta x}\right) - \left(\frac{f(x_{n+1}) - f(x_n)}{\delta x}\right)\right] \\
&= \frac{1}{\delta x^2}\Big(f(x_{n+2}) - 2f(x_{n+1}) + f(x_n)\Big)
\end{aligned} \tag{3.32}$$

while the backward difference approximation is:

$$\begin{aligned}
\left[\frac{d^2f}{dx^2}\right]_n^- &:= \frac{f'(x_n) - f'(x_{n-1})}{\delta x} \\
&= \frac{1}{\delta x}\left[\left(\frac{f(x_n) - f(x_{n-1})}{\delta x}\right) - \left(\frac{f(x_{n-1}) - f(x_{n-2})}{\delta x}\right)\right] \\
&= \frac{1}{\delta x^2}\Big(f(x_n) - 2f(x_{n-1}) + f(x_{n-2})\Big)
\end{aligned} \tag{3.33}$$

both *eq(3.32)* and *eq(3.33)* have an error in the first order of the discretization step δx. The centered approximation can be computed as:

$$\begin{aligned}
\left[\frac{d^2f}{dx^2}\right]_n^0 &:= \frac{f'(x_{n+1}) - f'(x_{n-1})}{2\delta x} \\
&= \frac{1}{2\delta x}\left[\left(\frac{f(x_{n+2}) - f(x_n)}{2\delta x}\right) - \left(\frac{f(x_n) - f(x_{n-2})}{2\delta x}\right)\right] \\
&= \frac{1}{4\delta x^2}\Big(f(x_{n+2}) - 2f(x_n) + f(x_{n-2})\Big)
\end{aligned} \tag{3.34}$$

which can be achieved alternatively by applying the forward, then backward approximations or the other way around, as follows:

$$\begin{aligned}\left[\frac{d^2f}{dx^2}\right]_n^0 &:= \frac{f'(x_{n+1}) - f'(x_n)}{\delta x} \\ &= \frac{1}{\delta x}\left[\left(\frac{f(x_{n+1}) - f(x_n)}{\delta x}\right) - \left(\frac{f(x_n) - f(x_{n-1})}{\delta x}\right)\right] \\ &= \frac{1}{\delta x^2}\Big(f(x_{n+1}) - 2f(x_n) - f(x_{n-1})\Big) \end{aligned} \tag{3.35}$$

or

$$\begin{aligned}\left[\frac{d^2f}{dx^2}\right]_n^0 &:= \frac{f'(x_n) - f'(x_{n-1})}{\delta x} \\ &= \frac{1}{\delta x}\left[\left(\frac{f(x_{n+1}) - f(x_n)}{\delta x}\right) - \left(\frac{f(x_n) - f(x_{n-1})}{\delta x}\right)\right] \\ &= \frac{1}{\delta x^2}\Big(f(x_{n+1}) - 2f(x_n) - f(x_{n-1})\Big) \end{aligned} \tag{3.36}$$

eq(3.35) and *eq(3.36)* are equivalent to *eq(3.34)* if δx in the latest two expressions is doubled. The truncation error again is of order δx^2 as when equations *3.28* and *3.30* are substituted in *eq(3.36)* or its equivalent ones above, the approximation gives:

$$\left[\frac{d^2f}{dx^2}\right]_n^0 = \frac{d^2f(x_n)}{dx^2} + O(\delta x^2)$$

Time integration algorithm

In molecular dynamics simulations, the successive configurations of a system are obtained by integrating the equations of motion, i.e., Newton's second law. The resultant solution function (trajectories) describes obviously the change in positions and velocities of the moving particles over time. Under influence of continuous potentials, the force on each particle varies with its position as well as positions of some/all other particles; this coupled motion of particles gives rise to a complicated many-body problem. To cope with this difficulty, the equations of motion are numerically integrated using the simple, yet efficient method of finite difference discussed above. The trajectory of the system is a univariate function of time which is discretized into infinitesimally separated points on the time axis, such separation is of the order of the atomic unit of time, at least one order of magnitude less than the fastest motion (vibration) in the system. The choice of a small time step reduces both the truncation and the round-off errors [12], and that is why a time step in the order of a femtosecond is usual in most MD applications.

Numerical integration of the equations of motion of the interacting particles, requires the time integration algorithm. Such algorithms are based on the finite difference scheme

which is based on 'truncated' Taylor expansion at some terms. Once the positions and their first and second order time derivatives are known at some time (point on the grid), their equivalent quantities are computed by the integration algorithm. Among the so many time integration algorithms and most commonly used in MD is the Verlet integration algorithm, the basic idea is to consider a third order Taylor series expansion of the position $r(t)$ twice, one forward and one backward in time, similar to Eqs.(3.28 and 3.30)

$$r(t_{n+1}) = r(t_n) + \delta t \frac{d}{dt} r(t_n) + \frac{1}{2} \frac{d^2}{dt^2} r(t_n) \delta t^2 + \frac{1}{6} \frac{d^3}{dt^3} r(t_n) \delta t^3 + O(\delta t^4) \tag{3.37}$$

$$r(t_{n-1}) = r(t_n) - \delta t \frac{d}{dt} r(t_n) + \frac{1}{2} \frac{d^2}{dt^2} r(t_n) \delta t^2 - \frac{1}{6} \frac{d^3}{dt^3} r(t_n) \delta t^3 + O(\delta t^4) \tag{3.38}$$

the sum of *eqs 3.37* and *3.38* gives:

$$r(t_{n+1}) = 2r(t_n) - r(t_{n-1}) + a(t_n) \delta t^2 + O(\delta t^4) \tag{3.39}$$

where $a(t_n) = \dfrac{d^2}{dt^2} r(t_n) = -\dfrac{1}{m} \nabla V(r(t_n))$ is the acceleration of particle, and V is the potential energy surface. The error is shown to be of the order $O\delta t^4$ in eq 3.39. One can compute velocities from the positions by using the centered finite method as:

$$v(t_n) = \frac{d}{dt} r(t_n) = \frac{r(t_{n+1}) - r(t_{n-1})}{2\delta t} \tag{3.40}$$

This velocity expression is associated with an error of the order δt^2 rather than δt^4 which could affect the computations. However, some variants of the verlet algorithm have been developed: the leap-frog and the velocity Störmer-Verlet (the later is simply referred to as velocity Verlet).

The leap-frog is a modified version of the Verlet algorithm to obtain more accurate velocity expression than in *eq 3.40* and overcome thus the errors in the order δt^2, this is usually used when the kinetic energy is needed as for example in velocity scaling.

$$\begin{aligned} r(t_{n+1}) &= 2r(t_n) - r(t_{n-1}) + a(t_n)(\delta t^2) \\ &= r(t_n) + \left(\frac{r(t_n) - r(t_{n-1})}{\delta t} \right) (\delta t) + a(t_n)(\delta t^2) \\ &= r(t_n) + v(t_{n-\frac{1}{2}})(\delta t) + a(t_n)(\delta t^2) \\ &= r(t_n) + \Big(v(t_{n-\frac{1}{2}}) + a(t_n)(\delta t) \Big) (\delta t) \\ &= r(t_n) + v(t_{n+\frac{1}{2}})(\delta t) \end{aligned} \tag{3.41}$$

it is clear that, $v(t_{n-\frac{1}{2}}) = \left(\dfrac{r(t_n) - r(t_{n-1})}{\delta t} \right)$ is just the centered finite difference approximation of the first order time derivative of the position at the grid point $t_n - \frac{1}{2}$ at points half the time step away, similarly $v(t_{n+\frac{1}{2}}) = \Big(v(t_{n-\frac{1}{2}}) + a(t_n)(\delta t) \Big)$ is the centered finite

difference expression of $a(t_n)$ as the first order time derivative of $v(t_n)$ using again half time step.

In the velocity *Störmer* Verlet algorithm, positions, velocities and accelerations at some instant of time are obtained from their counterparts at the very earlier time instant (time step) as below shown:

$$r(t_{n+1}) = r(t_n) + v(t_n)(\delta t) + \frac{1}{2}\, a(t_n)(\delta t^2) \tag{3.42}$$

$$v(t_{n+\frac{1}{2}}) = v(t_n) + \frac{1}{2} a(t_n)(\delta t) \tag{3.43}$$

$$a(t_{n+1}) = -\frac{1}{m}\nabla V(r(t_{n+1})) \tag{3.44}$$

$$v(t_{n+1}) = v(t_{n+\frac{1}{2}}) + \frac{1}{2} a(t_{n+1})(\delta t) \tag{3.45}$$

where r, v, a, are the position, velocity and acceleration of the particle respectively.

Verlet algorithm as seen is not a self-starting, that is it depends on two sets of initial conditions of positions in two instants back in time where we have obviously one and only one set of initial positions and velocities, one way to overcome such a case is by using the truncated Taylor series:

$$r(t_{-1}) = r(t_0) + v(t_0)(\delta t)$$

to get the second set of positions at earlier times. The initial velocities at time t_0 can be set to zeros, hence $r(t_{-1}) = r(t_0)$, or assigned from a Maxwellian distribution at a certain temperature 'T'. In the later case, the velocities must have a zero mean and their variance is one, i.e., there no translational motion for whole system since the total linear momentum is zero. Such ambiguity does not occur in either the leap-frog or the velocity Verlet schemes as they take only one set of initial positions. One of the remarkable properties of Verlet algorithm is the time reversibility [47], i.e., under the transformation, $\Big(r\,(t+\delta t) \rightarrow r\,(t-\delta t)\Big)$, such algorithm is invariant. The forward and backward time evolution are equally possible to compute in principle using Verlet algorithms, whereas in practice round-off errors are the reason for numerical irreversibility.

3.2 *Ab initio* Molecular Dynamics

In situations when classical molecular dynamics breaks down or it becomes extremely inappropriate, in addition to the absence of one universal fixed interatomic potential model, *ab initio* Molecular Dynamics is used in intention to minimize the amount of fitting and guesswork. In the ab initio discipline, the electronic variables can not be integrated out, and the quantum nature of the very small electrons is considered by including their active

degrees of freedom. Forces on nuclei are then obtained from first principle electronic structure calculations for each generated molecular dynamics trajectory, and the subsequent nuclear trajectories are generated by solving Newton's equations of motion on the ground state electronic surface. Some case examples where ab initio approach is devised, are:

1. Effects of finite temperature.
2. Non-trivial reaction coordinates.
3. Materials properties under high pressure and high temperature.
4. Bond making, bond breaking and any corresponding qualitative change in bonding.
5. Systems of many different types of atom where there are many different interatomic interactions that have to be parameterized.

Though the ab initio schemes are advantaged with accuracy over the classical approach, they are still limited to small systems (hundreds to thousands of atoms) and to short time dynamics and/or sampling times. Those limits are due to the difficulty to handle the many electron system, and to select an appropriate approximation for solving the Schrödinger equation.

In the following, we would briefly describe the three variants of ab initio methods, namely: Born-Oppenheimer, Ehrenfest and Car-Parrinello Molecular Dynamics. For more detailed discussions, see Refs([27, 28]).

3.2.1 Born-Oppenheimer Molecular Dynamics

Born-Oppenheimer Molecular Dynamics considers the quantum nature of electrons by solving the electronic time-independent Schrödinger equation for each time step, i.e., each nuclear configuration, where the time-dependence of the electronic structure is included only via the nuclear motion. The time evolution of the system in the electronic ground state, is described by the simultaneous numerical solutions of the following two equations

$$E_0^{\mathrm{BO}} = \min_{\Psi_0(r,R)} \left\{ \left\langle \Psi_0(r,R) \ |\mathcal{H}_e|\Psi_0(r,R) \right\rangle \right\} \tag{3.46}$$

where $\mathcal{H}_e$ was defined in Eq.(2.13). The classical dynamics of nuclei is described by

$$M_I \ddot{R}_I(t) = -\nabla_{R_I} \ E_0^{\mathrm{BO}} \tag{3.47}$$

3.2.2 Ehrenfest Molecular Dynamics

Ehrenfest TDSCF Molecular Dynamics method is identified by simultaneously solving Eqs.(3.12 and 3.14) numerically, with the assumption that the electronic subsystem remains in one single adiabatic state which is usually taken to be the ground state $\langle \Psi_g(r, R(t)) |$. The respective nuclear and electronic equations are :

$$M_I \ddot{R}_I(t) = -\nabla_{R_I} \langle \Psi_g(r, R(t)) | \mathcal{H}_e | \Psi_g(r, R(t)) \rangle \tag{3.48}$$

$$\imath\hbar \frac{\partial \Psi_g(r, R(t))}{\partial t} = \mathcal{H}_e(r, R(t)) \ \ \Psi_g(r, R(t)) \tag{3.49}$$

The point catches attention here is that self-consistent minimization (diagonalization) of Eq.(3.46) has to be performed in each time step, it is stated that in Ehrenfest method a wavefunction minimizing the electronic hamiltonian at the start will always be in its respective minimum when the nuclei evolve classically according to Eq.(3.48). This initial wavefunction is obtained by one-time self-consistent diagonalization. However, the time-independent electronic Schrödinger equation is solved in Born-Oppenheimer method, whereas it is the electronic time-dependent Schrödinger equation is to be solved. This difference is reflected in the size of the maximum timestep, i.e. in Born-Oppenheimer method the size of the maximum time step follows the nuclear motion, while in Ehrenfest Molecular Dynamics the electronic motion controls the time step in Ehrenfest Molecular Dynamics.

3.2.3 Car-Parrinello Molecular Dynamics

Car-Parrinello Molecular Dynamics is a method that allows the use of a big time step controlled by the nuclear motion, and at the same time takes into account the electronic time-evolution in a different fashion than solving electronic time-dependent Schrödinger equation. To clear the point we consider the following, the ground state energy of the electronic subsystem, $E_0 = \langle \Psi_0 | \mathcal{H}_e | \Psi_0 \rangle$, was shown to be a function of nuclear positions R, it can be considered also as a functional of the total wavefunction Ψ_0, if this wavefunction is expanded in time-dependent one-particle basis set (orbitals); E_0 is then a functional of those orbitals $\{\psi_i(r,t)\}$. This way, forces on orbital would be computed in analogy to forces on nuclei as functional derivatives of a Lagrangian function with respect to the orbitals themselves. R. Car and M. Parrinello proposed, in their famous 1985 paper "Unified Approach for Molecular Dynamics and Density-Functional Theory[9] ", the following Lagrangian for a molecular system

$$\mathcal{L}_{cp} = \sum_I^N \frac{1}{2} M_I \dot{R}_I^2 + \sum_i^n \frac{1}{2} \mu_i \langle \dot{\psi}_i | \dot{\psi}_i \rangle - \langle \Psi_0 \ | \mathcal{H}_e | \Psi_0 \rangle + \text{constraint} \tag{3.50}$$

where μ_i is the fictitious mass assigned to the i-orbital, and it has units of energy times a squared time since orbitals are unitless. The constraint, e.g. orthonormality, within the total wavefunction might be a function of both R, and $\{\psi_i\}$, and will lead to a constraint dynamics. The Newtonian equations of motion, obtained from Euler-Lagrange equations, for nuclei and orbitals are

$$\frac{d}{dt}\left(\frac{\partial \mathcal{L}}{\partial \dot{R}_I}\right) = \frac{\partial \mathcal{L}}{\partial R_I} \tag{3.51}$$

$$\frac{d}{dt}\left(\frac{\delta \mathcal{L}}{\delta \dot{\psi}_i^\star}\right) = \frac{\delta \mathcal{L}}{\delta \psi_i^\star} \tag{3.52}$$

that is, the Car-Parrinello equations of motion for nuclei and orbitals are

$$M_I \ddot{R}_I(t) = -\nabla_{R_I}\langle \Psi_0 | \mathcal{H}_e | \Psi_0 \rangle + \nabla_{R_I}(\text{constraint}) \tag{3.53}$$

$$\mu_i \ddot{\psi}_i = -\frac{\delta}{\delta \psi_i^\star}\langle \Psi_0 | \mathcal{H}_e | \Psi_0 \rangle + \frac{\delta}{\delta \psi_i^\star}(\text{constraint}) \tag{3.54}$$

Have the system's ground state wave function been at a given time known, the dynamical behavior of that system is followed with the help of Eqs.(3.53, 3.54) which describe the simultaneous and concurrent propagation of electrons (orbitals) and nuclei. Iteration of the electronic structure problem would not be needed as long as the coupling (kinetic energy transfer) is small between nuclei and electrons. When the fictitious kinetic energy

$$\left(\sum_i \mu_i \langle \dot{\psi}_i^2 | \dot{\psi}_i^2 \rangle\right)$$

of the orbitals is low, electrons remain in their instantaneous ground state on the Born-Oppenheimer surface, still the orbitals' fictitious kinetic energy must be hight enough so that electrons adiabatically respond to the nuclear motion. General and deeper insights on the Car-Parrinello method are also provided in reference [44], in addition to the previously mentioned references [27, 28].

Chapter 4

Interatomic Potential Modeling

We start this chapter by a description of the interatomic interactions along with their assumed nature and how forces are related to a pre-defined scaler potential energy function. Then a historical overview of the design development of the potential model interactions is followed. In the second section we provide an intensive description of two major approaches of potential modeling for covalent systems, we discuss afterwards possibilities on how to add new features in those two forms of potential so to differentiate between the two diamond structures described in Chap.(6).

4.1 Many-body potential Models

It was only the electrostatic interactions considered in the molecular Schrödinger equation. It is further assumed that the expectation value of the electronic hamiltonian Eq.(2.10) describes a conservative interatomic potential, i.e. interactions are path independent and irrotational. Then interatomic forces can be within the above assumption evaluated as the gradient of that scaler interatomic potential function V(R), where ($R \equiv \{R_1, R_2, \ldots, R_N\}$) is the set of positions of the N nuclei in the system

$$F_{R_I} = -\nabla_{R_I} V(R_1, R_2, \ldots, R_N)$$

Since a conservative potential is invariant under translation and rotation, the corresponding equations of motion are also invariant, and their solutions are unique for the same set of initial conditions in all inertial frames. Lengths and angles under rotation and translation are preserved, and the potential functions can be expressed in terms of their relative position coordinates.

$$V = V(r_{12}, \cdots, r_{1N}, r_{IN}, \cdots, r_{N,N-1})$$

The potential function is furthermore expanded to pair-wise, three-body, and up to many-body contributions which are moreover categorized as intermolecular long-range and in-

tramolecular short-range interactions, see Eq.(3.25)

$$V(R) = \sum_{i<j} V_2(r_{ij}) + \sum_{i<j<k} V_3(r_{ij}, r_{ik}, r_{jk}) + \sum_{i<j<k<l} V_4(r_{ij}, r_{ik}, r_{il}, r_{jk}, r_{jl}, r_{kl}) + ... \quad (4.1)$$

where R is the atomic configuration. The expansion above is practically truncated at some term to reduce the dimensionality resulting from the increasing number of active nuclear degrees of freedom, where higher-order interactions would be instead effectively modeled.

In the early days of Molecular Dynamics, only pair potentials were mostly used, specially Morse and Lennard-Jones formulae. While Morse potential describes bonding in diatomic molecules, the model of Lennard-Jones describes approximately the isotropic (non-directional and only distant-dependent) parts of van der Waals (long-range attractive dipolar) and short-range repulsive forces, and usually parametrized in the '6-12' form

$$V_0(r) = -\frac{A}{r^6} + \frac{B}{r^{12}} \quad (4.2)$$

where A and B are positive constants. The isotropic character of the two former potentials would limit their outcomes only to highly symmetric close-packed structures, i.e. structures of a minimized surface and a maximized number of neighbors.

Generally, all analytical pair potentials describe only the isotropic parts of interactions. They would moreover predict hexagonal close-packed structures. The cubic close-packing nature of Argon could be predicted by using Dymond-Alder numerical pair potential [11]. Experiments provide however that, except helium, nobel gas crystals are cubic close-packed with roughly 0.001 deeper energy minimum than if they would have been hexagonally close-packed. The interplay between experimental and pair potential outcomes was stated in Ref.([38]) as follows:

> *"Some of the earliest experimental evidence for many-body interactions comes from the noble gas solids. The most accurate nobel gas pair potentials incorrectly predict a hexagonal close-packed structure, and crystal binding energies indicate approximately 10% deviations from the pairwise additivity."*

One of the earliest attempts to model the anisotropic many body interaction was by Axilrod and Teller. In their formula[4], a triple-dipole dispersive interaction was proposed via the following three-body correction term.

$$V_{123} = \epsilon_0 \left[\frac{1 + 3\cos(\gamma_1)\cos(\gamma_2)\cos(\gamma_3)}{\left(r_{12} r_{13} r_{23}\right)^3} \right] \quad (4.3)$$

where γ_n is the angle subtended at atom n, and ϵ_0 is a positive parameter.

In metallic solids, atoms are held together by the co-called metallic bonds. This type of bonding is identified by molecular orbitals delocalized over all atoms where the valence electrons in those orbital are shared among all nuclei. The whole structure is bound due to the isotropic coulomb attraction between those delocalized valence electrons and positive cores. The isotropy in metallic bonding leads to closed-packed structures that maximize both space filling and coordination number, i.e. number of closest neighbors.

Ionic bonds in analogy are characterized by the highly localized molecular orbitals, and stability of the ionic structures are attributed to the electrostatic attraction between the opposite ions in the solid. Ionic solids are also expected to form closed packed structures, however the relative size of the cation and anion seems to have influence on the coordination number[35]. In a brief prospective, the many body effects in ionic or metallic system are usually introduced in functional form of the coordination number of an atom. Physically, it takes into account the effects of the local environment of the atom i.e. the bigger the coordination number is (or the more the neighbors are), the weaker the bonds become as a consequence of Pauli exclusion principle.

Structures in which atoms have a low coordination number, less or equal to 4, provide evidence for a dominant role of the highly directional covalent bonding among nearest neighbors. A weaker directional character is also evident for hydrogen bonding and dipole-dipole interactions, and its absence in pair potentials, i.e., the absence of many body effects, makes pair potentials inappropriate to simulate open structures such as the tetrahedral based diamond for example. Stillinger and Weber have stated this clearly as follows:

> *"No reasonable pair potential will stabilize the diamond structure, as V_{LJ} stabilizes the close-packed crystals characteristics of the noble gases."*

They, Stillinger and Weber, have in 1985 constructed a potential formula, Sec.(4.2.1), that has a three-body term which models the directionality in the covalent net of diamond by including explicit dependency on the bond angle, i.e., the angle between two bonds centered at one atom.

$$V = \sum_{i<j} V_2(\{r_{ij}\}) + \sum_{i<j<k} V_3(\{r_{ij}\}, \{\theta_{ijk}\}) \tag{4.4}$$

where $\theta = 109.5°$ is the angle of a minima.

Some atoms adapt themselves to different environments in different structures, this is the idea behind the environment dependent interaction potential (EDIP)[17] and its extended or generalized form[26]. EDIP can be thought of as a modified version of Stillinger-Weber formulation, where both the two-body and the angular three-body contributions depend on the configuration of the atoms, i.e. on the number of neighbors, where the later is included in the potential with the help of a continuous switching cutoff function.

Chemistry of atoms is confirmed such that competing bonds on one atom weaken each other, i.e., a bond to a central atoms is weaker if the same atom forms another bond with another atom. This is the central idea of the Bond Order Potential (BOP). BOP is simply written as a pair interactions with coefficients of either attraction, repulsion or both are no longer constant but modified by the local environment of each atom, i.e.,

$$V_{ij} = V_{ij}^{r}(r_{ij}) \sum_{k} A_{ij}(\{r_{ij}\},\{\theta_{ijk}\}) + V_{ij}^{a}(r_{ij}) \sum_{k} B_{ij}(\{r_{ij}\},\{\theta_{ijk}\}) \tag{4.5}$$

where A_{ij} and B_{ij} are the strength of repulsion V_{ij}^{r} and attraction V_{ij}^{a} respectively and they are functions of the atom's local environment, see Sec.(4.2.2). B_{ij} is described as a three-body interactions, and usually short ranged to the nearest neighbors of the atom, analysis reveals that a 4-body term can be strengthen by controlling the range of interactions, see Sec.(4.2.3).

4.2 Potential models for covalent systems

In contrast to metallic and ionic systems, the anisotropic interactions in covalent structures do not maximize the space filling, this is a consequence to the low coordination number characterizes the covalent interactions. In what follows we will discuss two potential formulas representing anisotropic potential energy-surface, and mark their basic approach to simulate covalent systems. We would also describe how possible to effectively include a four-body interactions i.e. effects of the so called dihedral dependences.

4.2.1 Stillinger-Weber potential

Stillinger and Weber potential defined their potential formula[36] as follows:

$$\Phi(\mathbf{r}_1,\mathbf{r}_2,\mathbf{r}_3,....,\mathbf{r}_N) = \sum_{i<j} v_2(\mathbf{r}_i,\mathbf{r}_j) + \sum_{i<j<k} v_3(\mathbf{r}_i,\mathbf{r}_j,\mathbf{r}_k) + ... \tag{4.6}$$

Introduce energy and length units, ε and σ,

$$\begin{aligned} v_2(\mathbf{r}_i,\mathbf{r}_j) &= v_2(r_{ij}) = \varepsilon f_2(r_{ij}/\sigma) \\ v_3(\mathbf{r}_i,\mathbf{r}_j,\mathbf{r}_k) &= \varepsilon f_3(\mathbf{r}_i/\sigma,\mathbf{r}_j/\sigma,\mathbf{r}_k/\sigma) \end{aligned} \tag{4.7}$$

$$f_2(r) = \begin{cases} A(Br^{-p} - r^{-q})\exp\left[(r-a)^{-1}\right], & r < a \\ 0, & r \geq a \end{cases} \tag{4.8}$$

$$f_3(\mathbf{r}_i, \mathbf{r}_j, \mathbf{r}_k,) = h(r_{ij}, r_{ik}, \theta_{jik}) + h(r_{ji}, r_{jk}, \theta_{ijk}) + h(r_{ki}, r_{kj}, \theta_{ikj}) \tag{4.9}$$

where θ_{ijk} is the angle between $\mathbf{r}_{ji}$ and $\mathbf{r}_{ki}$, at the vertex i. The functions h have two parameters, $(\lambda, \gamma) > 0$, which is nonzero only if both $r_{ij} < a$ and $r_{ik} < a$

$$h(r_{ij}, r_{ik}, \theta_{jik}) = \lambda \exp\left[\gamma(r_{ij} - a)^{-1} + \gamma(r_{ik} - a)^{-1}\right] \quad \left(\cos\theta_{jik} + \frac{1}{3}\right)^2 \tag{4.10}$$

and identically equal to zero outside of these two conditions.

They made a limited search, their parameters:

$$A = 7.049556277, \qquad B = 0.6022245584$$

$$p = 4, \qquad q = 0, \qquad a = 1.80$$

$$\lambda = 21.0, \qquad \gamma = 1.20,$$

with units in Ångström and electronvolt.

4.2.2 Tersoff's potential

Based on Abell's work[1], J. Tersoff constructed in 1988 a potential formula for elemental covalent systems[42], a modified version of his earlier formulation found in Ref.([40]) , this formula is based on the chemical concept of bond order introduce by Linus Pauling. Bond order potential considers the influence of the closet neighbors to one atom on its bonding strength. The bond strength in Tersoff's model includes the effect of the angular configuration of the covalently bonded atoms, i.e., the characteristic directional nature of the covalent bonds. The proposed potential is:

$$\begin{aligned} E &= \frac{1}{2}\sum_{\substack{i=1 \\ j\neq i}}^{N} V_{ij} \\ V_{ij} &= f_c(r_{ij})[a_{ij}\ f_{\mathrm{R}}(r_{ij}) - b_{ij}\ f_{\mathrm{A}}(r_{ij})] \end{aligned} \tag{4.11}$$

where

$$\begin{aligned} f_{\mathrm{R}}(r) &= A\ \exp(-\lambda_1\ r) \\ f_{\mathrm{A}}(r) &= B\ \exp(-\lambda_2\ r) \end{aligned} \tag{4.12}$$

are the repulsive and attractive interactions respectively, and$f_c(r)$ is an appropriate cut-off function defined by Tersoff as:

$$f_c(r) = \begin{cases} 1, & r < R - D \\ \frac{1}{2} - \frac{1}{2}\sin[\frac{\pi}{2}\frac{(r-R)}{D}], & R - D < r < R + D \\ 0, & r > R + D \end{cases} \tag{4.13}$$

The term a_{ij} represents the repulsion strength, and its proposed form is:

$$\begin{aligned} a_{\imath\jmath} &= [1 + (\alpha\eta_{\imath\jmath})^n]^{-\frac{1}{2n}} \\ \eta_{\imath\jmath} &= \sum_{\substack{k\neq\imath \\ k\neq\jmath}} f_c(r_{\imath k})\ \exp[\lambda_3^3(r_{\imath\jmath} - r_{\imath k})^3] \end{aligned} \tag{4.14}$$

when α is sufficiently small, $a_{ij} \approx 1$. Tersoff set α to zero so that $a_{ij} = 1$, i.e., repulsion between two atoms is not influenced nor modified by the presence of other atoms. Similarly, the $b_{\imath\jmath}$ term represents the attraction strength whose form is:

$$\begin{aligned} b_{\imath\jmath} &= [1 + (\beta\zeta_{\imath\jmath})^n]^{-\frac{1}{2n}} \\ \zeta_{\imath\jmath} &= \sum_{\substack{k\neq i \\ k\neq j}}^{N} \zeta_{\imath\jmath k} \\ \zeta_{\imath\jmath k} &= f_c(r_{\imath k})\ g(\theta_{\imath\jmath k})\ \exp[\lambda_3^3(r_{\imath\jmath} - r_{\imath k})^3] \\ g(\theta) &= 1 + \left(\frac{c}{d}\right)^2 - \frac{c^2}{d^2 + [h - \cos(\theta)]^2} \end{aligned} \tag{4.15}$$

note that, unless the two atoms $\imath$ and $\jmath$ have exactly similar local surroundings 'environments', $b_{\imath\jmath} \neq b_{\jmath\imath}$, i.e., the bonding strength has in general asymmetric formulation.

Parameters for Carbon as given in [41] are:

A (eV)	1393.6	n	0.72751
B (eV)	346.74	c	38049
λ_1 (Å^{-1})	3.4879	d	4.3484
λ_2 (Å^{-1})	2.2119	h	-0.57058
λ_3 (Å^{-1})	0	R (Å)	1.95
β	1.5724 $\times 10^{-7}$	D (Å)	0.15

Tersoff himself has extended his model where he proposed a general form to treat the heteronuclear bonds for multicomponent system[43].

Brenner showed in [6] that under a reasonable choice of the functionals and parameters, the expressions of both the embedded-atom method, developed by Daw and Baskes, and that of Tersoff model are identical. Furthermore Brenner [7] indicated the nonphysical behavior resulting from interaction between a 4-coordinated and another 3-coordinated Carbon atoms where bonding in such a case is better described as over-binding of radicals. The absence of a nonlocal effects ,e.g., conjugated and non-conjugated bonding would also lead to a physical inconsistency. In attempt to correct both problems above and simultaneously keep the fit of Tersoff's formula, he proposed a sum over bonds in Eq.(4.11), and introduced a nonlocal term, to diversify conjugated and non-conjugated systems, in the attraction strength which is then averaged as follows

$$b_{ij} = \frac{b_{ij} + b_{ji}}{2}$$

For the case of hydrocarbons as well as Carbon systems, he has introduced a new empirical potential expression based on the Abell-Tersoff empirical bond order formalism. For more information on his formula, the reader is referred to [7]. A second-generation potential energy function [8] based on the bond order formalism was later proposed, by Brenner and coauthors, for solid carbon and hydrocarbon molecules. According to Brenner, the new approach allows a classical description of covalent bond breaking and forming along with the associated changes in atomic hybridization.

4.2.3 The four body correlations and the cut-off features

A large number of simulations is based on the so called bond-order potentials, mainly the Tersoff and Brenner versions. These potentials are highly empirical, based originally on the concept of bond order, i.e. the presence of other atoms (bonds) influences the strength of the individual terms of the potential. The potential energy, giving rise to the individual forces, assumes a full summation over all of the constituents, in practice limited by the cut-off properties of the model. This limit marks this potential essentially as a three-body interaction model, i.e. it would not, similar to Stilinger-Weber formula, distinguish between structures that have different four-body configurations (dihedral angles), e.g the structures of diamond and lonsdaleite. In this part we have studied critically the current versions of these potentials, with respect to how they can and how they in fact do incorporate the desired physical features of the atomic systems in question. In our studies we have first noticed a somewhat unexpected strong dependence on the cut-off parameters, in fact as illustrated for the case two atoms in Fig.(4.1), the main attractive forces are determined by the derivative of the cut-off function. This is not a serious problem in principle, since all the parameters have been found appropriate in the rich spectrum of applications, but we are rather pointing to the possibility of greatly simplifying the mathematical functions used.

The most important question we have been pursuing is how the very complex mathematical form incorporates the structural features, as visualized by the angles between the bonds, and related further geometrical features.

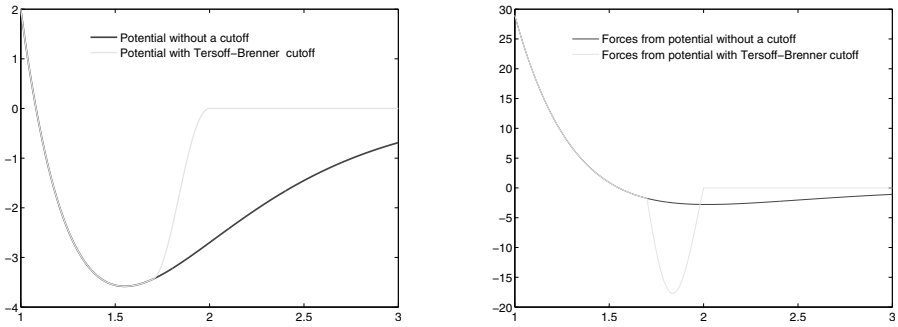

(a) Role of the cutoff in potential between two atoms.

(b) Role of the cutoff in the force between two atoms

Figure 4.1: Cutoff role in Tersoff-Brenner formalism

The cut-off function used in most Tersoff-Brenner applications is the cosine-type cut-off (4.13) which does not have a smooth derivative. In all our work it was replaced by the everywhere smooth and infinitely differentiable Fermi function

$$\frac{1}{\exp(\frac{r-\mu}{\nu})+1} \tag{4.16}$$

the parameter ν can be easily adjusted. Fig.(4.2) shows the comparison of the two cut-off features, and Fig.(4.3) shows how to control the Fermi cutoff, where the parameters $\mu = (R_2 + R_1)/2$ and $\nu = (R_2 - R_1) * \frac{\pi}{20}$ in Eq.(4.16), and the parameters $R = \frac{R_1+R_2}{2}$ and $D = \frac{R_2-R_1}{2}$ in Eq.(4.13).

The geometry hidden in Tersoff potentials is of the same type as in Stillinger-Weber formula, i.e. the angle must be close to the "preferred" angle ($\theta^0 = \cos^{-1}(h = -0.57058) \sim 124.7907°$) which minimizes the angular function in Eq.(4.16). Since only one angle is however included, how can Tersoff-Brenner potentials generate both graphene and diamonds? We believe this is a consequence of the topological properties of the Euclidean space as a second factor, i.e. a slight deviation from the preferred angle θ^0 results in only a slight change in the attraction strength, it is rather possible to build up both structures due to the fact that hexagons (angle 120°) cover the plane, and highly ordered tetrahedral-based geometry (angle of 109.5°) results in hexagonal and cubic diamonds in the 3-dimensional space. Similarly, the angle of a regular pentagon (108°) would result if atoms are arranged in a spherical shell, as it is the case of Buckminsterfullerene (C_{60}).

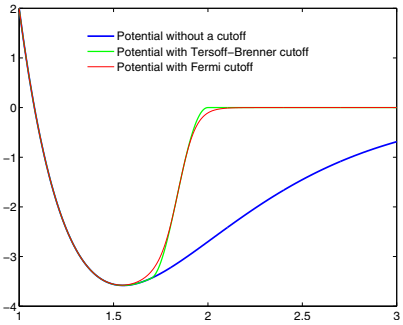

(a) Comparison between Tersoff-Brenner cutoff and the Fermi cutoff in the potential.

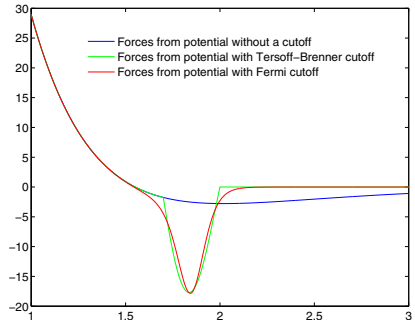

(b) Comparison between Tersoff-Brenner cutoff and the Fermi cutoff in the force.

Figure 4.2: Tersoff-Brenner cutoff and Fermi cutoff

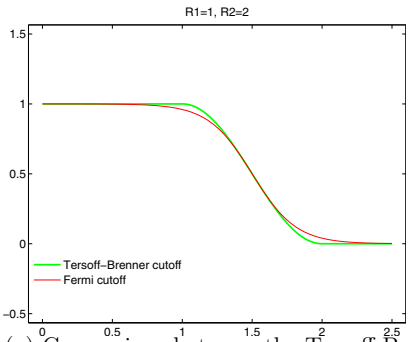

(a) Comparison between the Tersoff-Brenner and Fermi cutoffs

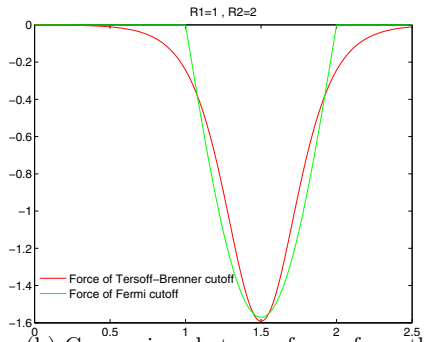

(b) Comparison between forces from the Tersoff-Brenner and Fermi cutoffs

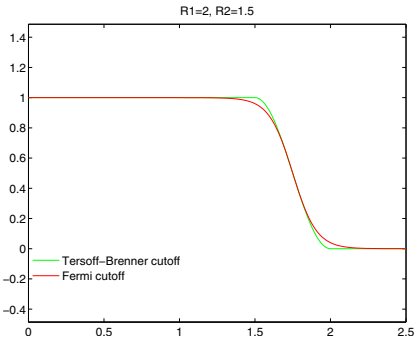

(c) Comparison between the Tersoff-Brenner and Fermi cutoffs

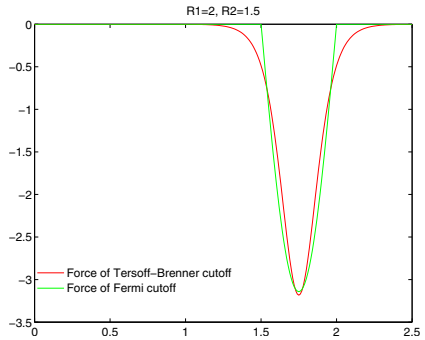

(d) Comparison between forces from the Tersoff-Brenner and Fermi cutoffs

Figure 4.3: Controlling the Fermi cutoff

Carbon atom in both diamond and lonsdaleite structures has up to the first neighbors a completely identical environment. The interaction with the nearest neighbors can be sufficiently well represented by a three-body interaction of as simple type as the Stillinger-Weber ,Tersoff-Brenner potentials contain in principle more complex correlations. The angular features in the Tersoff-brenner potential concern only the bond angle, i.e. the bonding strength b_{ij} is maximized for the (ijk)-triple when the angle θ_{ijk} is close to the value of $\theta_0 = \cos^{-1}(h)$, see Eq.(4.16). However diamond and lonsdaleite differ one another in the four-body configuration (dihedral angle), only the 60° dihedral angle (staggered configuration) appears in diamond whereas lonsdaleite has both the staggered and the eclipsed (0° dihedral angle) configurations. The difference in diamond family structures can be seen by the aliphatic type and boat type chains, see the figure 4.4. To differentiate between those two different 4-atom conformations in the two discussed structures, a 4-body correlation must be made effective in the interaction model. Due to the implicit sum

(a) The armchair chain characterizes lonsdaleite.

(b) The aliphatic chain in both lonsdaleite and diamond

Figure 4.4: Carbon Chains in diamond polymorphs

over all triplets in the bond strength of the Tersoff-Brenner potentials, one would expect the possibility to have a 4-body correlation. However, with the cut-off function used in the standard formulation, the mutual influence is limited to the nearest neighbors, and the standard cut-off prevents any higher than a 3-body correlation. If repulsion would be allowed to act over a longer range, using a different cut off for each of the two terms, one could in principle model a four body correlation using only 3-body interactions without any other modifications of the Tersoff-Brenner model, see Fig.(4.5).

There is no particular reason why the repulsion and attraction parts should have identical range, but it remains to be tested how extensive modifications to the whole model would be needed to implement such changes of the cut-off feature. Without any such modification, Both Tersoff-Brenner and Stillinger-Weber interactions lead to a situation where both diamond and lonsdaleite are energetically completely equivalent. The effective four-body

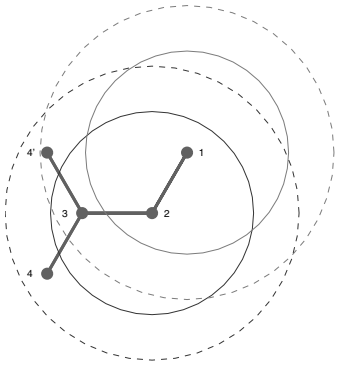

The cut-off role in effectively modeling a four body correlation for Tersoff-Brenner formula. The solid red line does not distinguish between atom 4 or $4'$ seen from atom 1, whereas the dashed red line indicates the difference. Both blue lines indicate no difference in three-body terms 234 and $234'$ seen from atom 2, i.e. the components $\zeta_{324} = \zeta_{324'}$, see Eq.(4.16)

Figure 4.5: 4-body correlations

effect due to a longer repulsion discussed here for the Tersoff-Brenner case would give a similar effect also in the case of the Stillinger-Weber formula, even without introducing a new explicit 4-body term. With this same approach, lonsdaleite would become energetically less favorable than diamond, which is a desirable result, both from observation and from calculations, see reference [31]. The above suggested procedure can be used to diversify any two 4-body configuration, it is a matter of what range in which the cut-off function is active.

The effective four-body interaction modeled this way is at the expenses of getting the an energy barrier as seen in Fig.(4.6). This energy hump can probably be interpreted as the amount of energy needed to form or break the chemical bond between two atoms since this hump is negligible when the all bonded neighbors are considered. Reference [34] provides a similar attitude to effectively model implicitly all angular features by only using an isotropic pair potential.

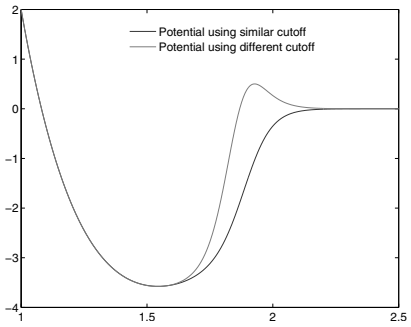

(a) The hump in the potential.

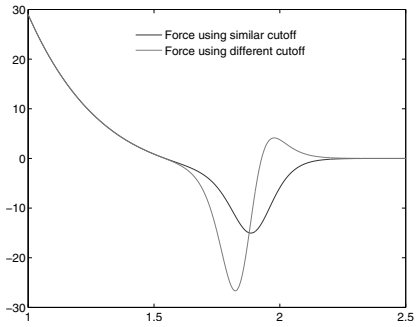

(b) The hump in the force.

Figure 4.6: Energy barrier and the shape of the force

Finally we show why Tersoff-Brenner formalism is not additive, and why the functional forms are always an exponential. The many-body interaction in Tersoff approach can be rewritten in the general form

$$V(r_1, r_2, \ldots\ldots r_N) = \frac{1}{2}\sum_{i}^{N}\sum_{j;j\neq i}^{N} F_{ij}\left(\sum_{k\neq i,j}^{N} G(r_i, r_j, r_k)\right)$$

One can imagine that this form is a result of a certain summation of this type of series:

$$\begin{aligned} V(r_1, r_2, \ldots\ldots r_N) &= \sum_{i,j;i<j}^{(pairs)} P_{ij}\,(r_i, r_j) + \sum_{i,j,k}^{(triplets)} T_{ijk}(r_i, r_j, r_k) \\ &\quad + \sum_{i,j,k,m}^{(quadruplets)} Q_{ijkm}(r_i, r_j, r_k, r_m) + \ldots \end{aligned} \tag{4.17}$$

in the sense described by Stillinger and Weber. However, only special types of the latter general expansion when summed would result into the former type of expression.

Chapter 5

Some programing aspects for molecular dynamics

We describe herein some of the aspects we have constantly used in programming Molecular Dynamics codes for investigation and explorations. The first is the fact that not all terms of geometrical quantities or forces are unique, thus they need not be directly calculated. The second is somehow related, for a short-range potential only some pairs in the system interact and again we do not need compute the zero-terms, those undesired terms are excluded by application of the soon described Verlet list. The third is the application of the periodic boundary conditions which serves to exclude effects of both the surface and the finite number of particles in the simulation.

5.1 Symmetry and antisymmetry

When coding a MD program, the first aim is to calculate all the relevant geometrical quantities (GQ), e.g., distances, angle, for the configuration of points, the set of their positions at a time instant. These GQ are furthermore substituted in some functional formula representing the intermolecular interaction potential. The corresponding forces are then computed by applying the analytical gradient on that potential energy surface. Forces are afterwards used to generate the new set of positions, configuration of points, at a later time instant using an appropriate time integration algorithm. This circular procedure is repeated over and over again, once per each time step in such a code.

In attempt to gain a speed up, we used the fact that only the unique and completely independent terms of the GQs need to be computed, henceforth terms in the potential and forces are also unique and independent. Identification of such unique terms is done by means of exploitation of anti-symmetry and symmetry presented in the potential formula.

Other dependent or non-unique terms are generated by performing the proper sum or permutation over the respective indices.

There is at least one anti-symmetric relation that is always reflected in forces due to the notation convention used to describe the relative distances between any two points, i.e.,

$$\vec{r}_{ij} = \vec{r}_j - \vec{r}_i \tag{5.1}$$

reflects a linear dependency of forces one on others for each unique n-tuple of indices, $\{\imath_1\ \imath_2\ \imath_3\ \cdots\ \imath_n\}$; considering an n-body potential, V_n, the corresponding interaction term is expressed as

$$V_n \equiv V_{\imath_1\imath_2\imath_3\cdots\imath_n}\left(r_{\imath_1\imath_2}, r_{\imath_1\imath_3}, \cdots, r_{\imath_1\imath_n}; r_{\imath_2\imath_3}, \cdots, r_{\imath_2\imath_n}; \cdots, r_{\imath_3\imath_n}; \cdots; r_{\imath_{n-1}\imath_n}\right) \tag{5.2}$$

the corresponding forces are

$$\begin{array}{rcccccc}
-F_{(\imath_1)\imath_2\imath_3\cdots\imath_n} &=& \dfrac{\partial V_n}{\partial r_{\imath_1\imath_2}}\nabla_{\imath_1} r_{\imath_1\imath_2} &+& \dfrac{\partial V_n}{\partial r_{\imath_1\imath_3}}\nabla_{\imath_1} r_{\imath_1\imath_3} & \cdots & \dfrac{\partial V_n}{\partial r_{\imath_1\imath_n}}\nabla_{\imath_1} r_{\imath_1\imath_n} \\
-F_{\imath_1(\imath_2)\imath_3\cdots\imath_n} &=& \dfrac{\partial V_n}{\partial r_{\imath_1\imath_2}}\nabla_{\imath_2} r_{\imath_1\imath_2} &+& \dfrac{\partial V_n}{\partial r_{\imath_2\imath_3}}\nabla_{\imath_2} r_{\imath_2\imath_3} & \cdots & \dfrac{\partial V_n}{\partial r_{\imath_2\imath_n}}\nabla_{\imath_2} r_{\imath_2\imath_n} \\
-F_{\imath_1\imath_2(\imath_3)\cdots\imath_n} &=& \dfrac{\partial V_n}{\partial r_{\imath_1\imath_3}}\nabla_{\imath_3} r_{\imath_1\imath_3} &+& \dfrac{\partial V_n}{\partial r_{\imath_2\imath_3}}\nabla_{\imath_3} r_{\imath_2\imath_3} & \cdots & \dfrac{\partial V_n}{\partial r_{\imath_3\imath_n}}\nabla_{\imath_3} r_{\imath_3\imath_n} \\
\vdots & & \vdots & & \vdots & & \vdots \\
-F_{\imath_1\imath_2\imath_3\cdots(\imath_n)} &=& \dfrac{\partial V_n}{\partial r_{\imath_1\imath_2}}\nabla_{\imath_n} r_{\imath_1\imath_n} &+& \dfrac{\partial V_n}{\partial r_{\imath_2\imath_n}}\nabla_{\imath_n} r_{\imath_2\imath_n} & \cdots & \dfrac{\partial V_n}{\partial r_{\imath_{n-1}\imath_n}}\nabla_{\imath_n} r_{\imath_{n-1}\imath_n}
\end{array} \tag{5.3}$$

whose expressions are simplified to

$$\begin{array}{rcccccc}
-F_{(\imath_1)\imath_2\imath_3\cdots\imath_n} &=& \dfrac{\partial V_n}{\partial r_{\imath_1\imath_2}}\left(-\hat{r}_{\imath_1\imath_2}\right) &+& \dfrac{\partial V_n}{\partial r_{\imath_1\imath_3}}\left(-\hat{r}_{\imath_1\imath_3}\right) & \cdots & \dfrac{\partial V_n}{\partial r_{\imath_1\imath_n}}\left(-\hat{r}_{\imath_1\imath_n}\right) \\
-F_{\imath_1(\imath_2)\imath_3\cdots\imath_n} &=& \dfrac{\partial V_n}{\partial r_{\imath_1\imath_2}}\left(\hat{r}_{\imath_1\imath_2}\right) &+& \dfrac{\partial V_n}{\partial r_{\imath_2\imath_3}}\left(-\hat{r}_{\imath_2\imath_3}\right) & \cdots & \dfrac{\partial V_n}{\partial r_{\imath_2\imath_n}}\left(-\hat{r}_{\imath_2\imath_n}\right) \\
-F_{\imath_1\imath_2(\imath_3)\cdots\imath_n} &=& \dfrac{\partial V_n}{\partial r_{\imath_1\imath_3}}\left(\hat{r}_{\imath_1\imath_3}\right) &+& \dfrac{\partial V_n}{\partial r_{\imath_2\imath_3}}\left(\hat{r}_{\imath_2\imath_3}\right) & \cdots & \dfrac{\partial V_n}{\partial r_{\imath_3\imath_n}}\left(-\hat{r}_{\imath_3\imath_n}\right) \\
\vdots & & \vdots & & \vdots & & \vdots \\
-F_{\imath_1\imath_2\imath_3\cdots(\imath_n)} &=& \dfrac{\partial V_n}{\partial r_{\imath_1\imath_2}}\left(\hat{r}_{\imath_1\imath_n}\right) &+& \dfrac{\partial V_n}{\partial r_{\imath_2\imath_n}}\left(\hat{r}_{\imath_2\imath_n}\right) & \cdots & \dfrac{\partial V_n}{\partial r_{\imath_{n-a}\imath_n}}\left(\hat{r}_{\imath_{n-1}\imath_n}\right)
\end{array} \tag{5.4}$$

addition of Eqs.(5.4) yields

$$F_{(\imath_1)\imath_2\imath_3\cdots\imath_n} + F_{\imath_1(\imath_2)\imath_3\cdots\imath_n} + F_{\imath_1\imath_2(\imath_3)\cdots\imath_n} + F_{\imath_1\imath_2\imath_3\cdots(\imath_n)} = 0 \tag{5.5}$$

and clearly indicates, for each unique n-tuple, a dependency of one force term on all other terms, i.e., one needs to calculate $(n-1)$ terms where the $n-th$ term is simply negative

the sum of the last $(n-1)$ terms. In the special case of pair-wise interactions, the GQs are only the relative distances, and this anti-symmetric relation corresponds to Newton's third law. It is therefor authors consequently refer to such anti-symmetry as Newton's third law for n-interacting particles.

For any further existent symmetry or antisymmetry, only the unique permutations for the N-particles through n-wise (n-body) potential are to be considered. Using permutation on a multiset the number of unique terms of the GQs or potential terms is

$$\begin{aligned}\begin{pmatrix} N \\ n-S \end{pmatrix} \begin{pmatrix} N-(n-S) \\ S \end{pmatrix} &= \frac{N!}{(N-n+S)!\,(n-S)!}\,\frac{(N-n+S)!}{(N-n)!S!} \\ &= \frac{N!}{(N-n)!\,(n-S)!S!} \end{aligned} \tag{5.6}$$

where $\{S : 0 <= S <= n\}$ is the number of unique bins (places) per any index in the n-tuple of indices $\{\imath_1\ \imath_2\ \imath_3\ \cdots\ \imath_n\}$ which identify the n-indexed geometrical quantity and its corresponding term in the n-body potential interactions. In the case when $S = 0$, the number of unique permutation is

$$\frac{N!}{(N-n)!n!}$$

and it corresponds to a complete asymmetry. One of the three-indexed geometrical quantity we have frequently encountered is the angle cosine, see [paper 2]. In this case application of analytical gradient relative to each index uncovers the linearly-dependence eq.(5.5) among the resultant forces. The (valence) bond angle $\theta_{\imath\jmath k}$ subtended at the vortex $\imath$ has symmetry under the interchange (permute) of the other two indices $\jmath, k$, henceforth only half the angles of all triplets in the N-particles system must be computed. The formula describing the angle subtended at the vortex $\imath$

$$\cos(\theta_{\imath\jmath k}) = \hat{r}_{\imath\jmath}.\hat{r}_{\imath k} \equiv \hat{r}_{\imath k}.\hat{r}_{\imath\jmath} \tag{5.7}$$

exhibits symmetry under the interchange of the indices $\jmath$ and k. In a similar analogy, the formula

$$\sin(\theta_{\imath\jmath k}) = \hat{r}_{\imath\jmath} \times \hat{r}_{\imath k} \equiv -\hat{r}_{\imath k} \times \hat{r}_{\imath\jmath} \tag{5.8}$$

exhibits antisymmetry under interchanging the indices $\jmath$ and k. Thus in both cases $\{S = 2; n = 3\}$; and the number of unique angles is obviously

$$\frac{N!}{(N-3)!\,(3-2)!2!} = \frac{1}{2}\frac{N!}{(N-3)!}$$

and the total unique force terms of the N-particle system triplet-wise interaction defined as a functional of the angle cosine is

$$\frac{1}{2}\frac{N!}{(N-3)!}\,(n-1) = \frac{N!}{(N-3)!}$$

since $n = 3$. For a three particle system, $N = 3$, then the numbers of unique angles and forces are 3 out of 6 and 6 out of 18 respectively. Similar discussions on exploitation of symmetry and antisymmetry in three-body interactions are available in [24, 37] with a further implementation for parallel molecular dynamics coding.

5.2 Verlet Neighbor list [46]

For short-range potentials, not all the n-permutations of a tuple of indices represent a set of interacting particles since particles at a larger separation than a spatial cutoff radius do not interact. A further reduction in computation is simply by taking advantage of the a spatial cutoff function which allows preclude calculations of the expected zero-terms. To do so, it is constructed for each particle a neighbor list containing all particles that are within slightly a larger distance than the cutoff radius. This list is used for several consecutive

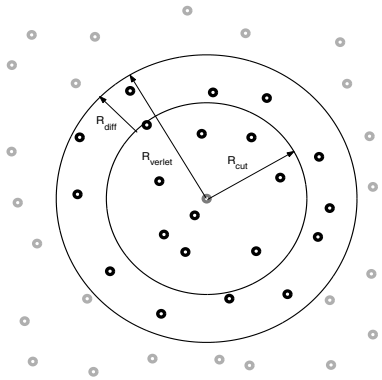

Figure 5.1: Graphical representation of Verlet Neighbor list
$R_{\text{diff}} = R_{\text{verlet}} > R_{\text{cut}}$

time steps before being updated. List update must be at the correct frequency, a common update is between 10 to 20 time steps. The greater R_{diff} is, the less frequent update of the neighbor list is required. To avoid double counting in the energy summation, only neighbors where $(\jmath > \imath)$ are stored. In some cases of three/four body interactions, it is a must to only exclude equal indices, i.e., the list must contain all the pairs $(\jmath \neq \imath)$ as it is clarified in [paper 1] for evaluation of three-body terms defined by the valence bond angle.

5.3 Boundaries

Restriction on the size of a time step is not the only challenge in molecular dynamics methods. Another concerns the finite size effects of the simulated system as its number of particles is far fewer than that in any natural sample, and is most from thousands to maximum few millions. Enclosing the system with a rigid-walled container, most particles would be under the influence of its boundaries through collisions. If we ignore the boundaries most particles would lie at surface whose area tends to be of minimized, distorting thus the shape of the system whenever it is a non-spherical. It is of no help to increase particles in a system as the more particles exist, the more particles are at the surface and more undesired effects are encountered. Those peculiarity due to the size limit and the improper treatment of boundaries, makes it unreliable to statistically extract macroscopic bulk properties since the later are calculated in the limit $N \to \infty$, where N is the number of particles. To go over both practical difficulties, periodic boundary conditions are imposed on the relatively small systems in such a way that particles experience forces as if they reside in the bulk.

5.3.1 Periodic boundary conditions (PBC)

When applying periodic boundaries, the fundamental (primitive) simulation cell is replicated infinitely and periodically in all directions. There is no restriction on the shape of the cell other than having the characteristic to completely fill all of space translationally with no overlaps nor voids. It is appropriate to choose a cell shape that reflects the underlying geometry of the system in question. When the interactions are of a short range each side of the replicated primitive cell must be of a length that is at least twice the radius of the spatial cutoff so to keep accuracy. Particles in this case are subjected to the condition such that when a particle leaves the primitive cell, its image from the cell on the opposite side reenters the cell with the same velocity. Herein, boundaries of the cell are no longer rigid but imaginary and their effects are completely absent. One must bear in mind when subjecting the system to this condition, the system is not any more invariant (symmetric) under space rotation, henceforth the angular momentum is no longer conserved whereas the linear momentum and mechanical energy are still conserved.

5.3.2 Minimum image convention for short range interactions

For short ranged forces, PBC are used in conjunction with the minimum image convention. In this scheme each particle interacts at most with only one image of every other particle

in the system. To exclude interactions of a particle with its own images (self-interaction), the assumed cubic simulation cell, as already mentioned, must have a side length of at least as twice as the radius of the cutoff. Interactions terms between pairs further away from each other than the cutoff radius are obviously zeros. Some three-body formulas are

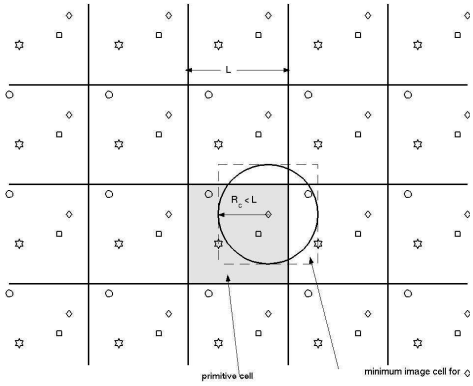

Figure 5.2: Graphical representation of Minimum image in 2D

expressed in terms of the three distances comprised by the triplet of interacting particles; considering the minimum image convention in these cases e.g. Axilrod-Teller potential[4], requires attention as the shape of the triangle formed by the interacting triplet must be kept contiguous. That is all the three relative distances must be within the cutoff range and must not be bigger than its radius, for more discussion on this point, readers are referred to [25, 49]. Such ambiguity is not encountered in programing Tersoff formula as the three-body term depends on only two distances rather than on the three, the geometrical shape formed by the triplet is the angle which is intuitively contiguous as long as the two distances from the vortex-particle to the other two particles at the ending points are within the cutoff range.

Chapter 6

Structural geometries

In this chapter, we introduce the after-the-fact orbital hybridization approach which is used to describe different structural geometries due to different bonding environments. Then we will describe different lattices in the following comparative prospective: graphene is introduced first; since it is widely used to describe many of the carbon elemental crystals, including graphite, fullerenes and nanotubes. Graphite is introduced second, and last is diamond. Then by using the so-called sphere close packing, we will provide a comparative description of geometrical aspects in two tetrahedral-based lattices for silicon, carbon and water ice.

6.1 Hybridization and Bonding in Carbon

To predict a molecular geometry and shape, the empirical-based VSEPR theory could be used. In this approach, ligands arrange themselves about the central atoms so as to maximize spherical symmetry. Though it works in some cases, it lacks any theoretical first principle justification. It does not model π-bonds nor does it give any information about either the electronic structure or the energetics of the system under investigation. For those reasons, two slightly different approaches, Molecular orbital (MO) theory and valence bond (VB) theory, were established on quantum bases. The concept of hybridization can be related to Linus Pauling's work and thus to VB, and it does beautifully describe the geometrical features for the different bonding phases of a two-, three- and four-coordinated central atom for a system in equilibrium.

The origin of the hybrid orbitals can be explained as follows: the $2s$ and $2p$ orbitals in one electron plus bare-nucleus atom, i.e. hydrogen-like atom, have the same energy. If we allow for the possibility of creating structures, i.e. give up the rotational symmetry so that the wavefunctions are not required to be eigenfunctions of angular momentum, we can

construct any combinations of these degenerate states. Since they have the same energy; any choice of a linear combination is as good as any other.

We start from sp hybridization orbitals, i.e. we assume that we want to keep $2p_z$ and $2p_y$ for themselves and make two completely equivalent combinations of the 2s and $2p_x$. This means, they should both have 50 per cent of each of the two. First we take the $2s$, $2p_+$, $2p_-$, and $2p_0$ and replace them with ϕ_s, ϕ_{p_x}, ϕ_{p_y}, and ϕ_{p_z}. The simple choices are

$$\psi_1^{sp_x} = \frac{1}{\sqrt{2}}(2\phi_s + 2\phi_{p_x}) \text{ , and } \quad \psi_2^{sp_x} = \frac{1}{\sqrt{2}}(2\phi_s - 2\phi_{p_x}), \text{ which is rewritten as :}$$

$$\begin{bmatrix} \psi_1^{sp} \\ \psi_2^{sp} \end{bmatrix} = \begin{bmatrix} \frac{1}{\sqrt{2}} & \frac{1}{\sqrt{2}} \\ \frac{1}{\sqrt{2}} & -\frac{1}{\sqrt{2}} \end{bmatrix} \begin{bmatrix} 2\phi_s \\ 2\phi_{p_x} \end{bmatrix}$$

The above wavefunctions are two sausages, one points in +x, the other in -x direction. The two remaining p_y and p_z are π-bonding orbitals, i.e., they allow the formation of π bonds neighboring atoms. Such hybridized states are found in carbon chains which has either alternating single and triple bonds or by cumulated double bonds [13, 45].

To further construct the sp^2 hybrid orbitals, we include $2s$, $2p_x$ and $2p_y$, and keep the out of plane $2p_z$ away. Each of the three new degenerate orbitals must have 33.3 percent of $2s$ since it does not have any geometrical direction, and 66.6% from the involved p-orbitals. We can start by combining $2s$ and $2p_x$ as before, but now with $\sqrt{\frac{1}{3}}$ and $\sqrt{\frac{2}{3}}$ as coefficients, and we can as well use the plus sign. It quickly turns out that the sp^2 hybridized orbitals (vectors) must be as follows:

$$\begin{bmatrix} \psi_1^{sp^2} \\ \psi_2^{sp^2} \\ \psi_3^{sp^2} \end{bmatrix} = \begin{bmatrix} \frac{1}{\sqrt{3}} & \frac{\sqrt{2}}{\sqrt{3}} & 0 \\ \frac{1}{\sqrt{3}} & -\frac{1}{\sqrt{3\times 2}} & \frac{1}{\sqrt{2}} \\ \frac{1}{\sqrt{3}} & -\frac{1}{\sqrt{3\times 2}} & -\frac{1}{\sqrt{2}} \end{bmatrix} \begin{bmatrix} \phi_s \\ \phi_{p_x} \\ \phi_{p_y} \end{bmatrix}$$

The sp^2 case has an angle of 120° between the geometrical directions of any two consecutive vectors. The possibility of p_z to form π bond gives rise to the energetically favorable planar geometry as it is the case in graphene.

In a similar manner, each degenerate sp^3 hybridized orbitals get $\frac{1}{4}$ of the ϕ_s orbital and an

over all of $\frac{3}{4}$ from the contributing p-orbitals.

$$\begin{bmatrix} \psi_1^{sp^3} \\ \psi_2^{sp^3} \\ \psi_3^{sp^3} \\ \psi_4^{sp^3} \end{bmatrix} = \begin{bmatrix} \frac{1}{\sqrt{4}} & \frac{\sqrt{3}}{\sqrt{4}} & 0 & 0 \\ -\frac{1}{\sqrt{4}} & \frac{1}{\sqrt{3}} \times \frac{1}{\sqrt{4}} & \frac{\sqrt{2}}{\sqrt{3}} & 0 \\ -\frac{1}{\sqrt{4}} & \frac{1}{\sqrt{3}} \times \frac{1}{\sqrt{4}} & \frac{\sqrt{2}}{\sqrt{3}} \times -\frac{1}{\sqrt{4}} & \frac{\sqrt{2}}{\sqrt{3}} \times -\frac{\sqrt{3}}{\sqrt{4}} \\ -\frac{1}{\sqrt{4}} & \frac{1}{\sqrt{3}} \times \frac{1}{\sqrt{4}} & \frac{\sqrt{2}}{\sqrt{3}} \times -\frac{1}{\sqrt{4}} & -\frac{\sqrt{2}}{\sqrt{3}} \times -\frac{\sqrt{3}}{\sqrt{4}} \end{bmatrix} \begin{bmatrix} \phi_s \\ \phi_{p_x} \\ \phi_{p_y} \\ \phi_{p_z} \end{bmatrix}$$

The resulting four vectors pointing towards the vertices of a regular tetrahedron are shown in figure(6.1) Thus we see that the tetrahedral structure of diamond can be traced to quite

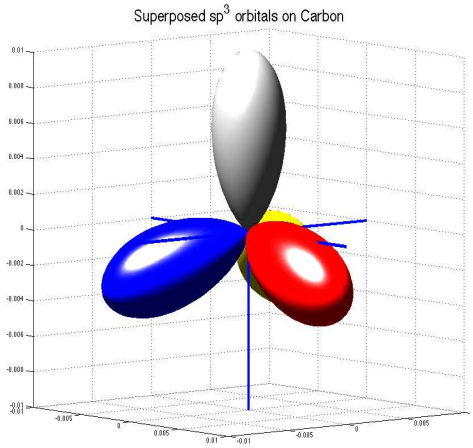

Figure 6.1: sp^3 Hybridized orbitals

elementary quantum mechanics. The requirement of energetically equivalent orbitals leads to both the hexagonal structure of graphite and the tetrahedral structure of diamond. The next point is the understanding of the built-up of the structure covering "whole space". We shall see that there are two possibilities, which are described by little intuitive terms "cubic diamond structure" and "hexagonal structure".

6.2 Crystal structures

Elemental carbon occurs in several allotropes, i.e different geometrical structures due to different local bonding environment. Information on carbon allotropes, some of their physical properties, and applications can be found in [13]. Such allotropes can be classified by means of the hybridization scheme. In that sense, carbon atom undergoes either sp^1, sp^2,

or sp^3 bonding configurations corresponding respectively to carbyne and polyyne, graphene and graphite, and diamond. Fullerenes and other nanostructures have in the major part an sp^2 hybridization state, but the arrangement of atoms on a spherical or cylindrical surface requires atoms to be in a mixed state between $sp^2 - sp^3$ hybridization as a response to the surface curvature. That is, space influences also the geometry of structures; it is known that hexagons do not cover a spherical surface, but twelve pentagons in addition to twenty hexagons will fit and cover beautifully the spherical surface of Buckyball. Similarly, carbon atoms in nanotubes are mainly in sp^2 hybridized state environment, but a small sp^3 hybridization proportions must exist.

Considering further neighbors of a carbon atom in crystalline arrays than its closest bonded ones, different arrangement and configurations of atoms are recognized. Crystals having the same bonding environment but have different configurations are known as polymorphs. Polytypes, being a special case of polymorphism, are variations of two or more polymorphs of the same element that are identical in two dimension but different in the third, i.e., they can be distinguished one from another by means of their layers' stacking sequences. That is, for our concern here spheres packing helps determine precisely the hybridization state and the overall geometry.

6.2.1 Graphene

Graphene Fig.(6.2), recently prepared as a unit apart in a free state [30], is a single sheet of carbon atoms arranged in regular benzene-like hexagonal rings. Each atom lies in a common vortex of three adjacent hexagons, and is covalently bonded to three atoms. The

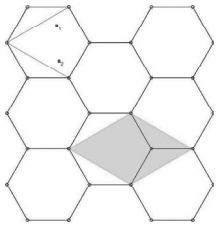

Graphene honeycomb lattice: the green rhombus is the non-primitive repeat unit cell of two lattice points, the red lines represent the lattice vectors $\vec{a}_1$ and $\vec{a}_2$, and the bond length is the same as basis vector $(\frac{\vec{a}_1}{3} + \frac{\vec{a}_2}{3})$. The red and blue colored circles show points of two different hexagonal lattices

Figure 6.2: Graphene honeycomb lattice

three bonds are equivalent and each has an order of $\frac{4}{3}$; this bond-order corresponds to one σ-bond and $\frac{1}{3}$ of a non-localized π-bond. The bond length is (1.42 Å), and the bond angle is (120°), this geometrical configuration is well understood in terms of the carbon sp^2 hybridized orbitals , Sec.(6.1). The remaining p-orbitals overlap together and form π-bonds delocalized over the whole sheet. Delocalization of the π-bonds is the reason behind both the planar geometry of graphene and the metallic behavior of heat and electric conductivity.

Even though silicon has a comparable electronic structure to that of carbon, silicon atoms do not aggregate into the planar structure of graphene, i.e they do not undergo sp^2 hybridization, the reason is that silicon-silicon σ-bonds are comparatively long, thus π orbitals can have a partial overlap which results in no energetic gain in forming π-bonds. Silicon atoms prefer instead the sp^3 tetrahedral arrangement described later.

In crystal notation, graphene has the well known honeycomb lattice which can be viewed as two interpenetrating bidimensional triangular (hexagonal) lattices, one is translated by $(\frac{\vec{a}_1}{3}+\frac{\vec{a}_2}{3})$ from the other, or equivalently as one bidimensional triangular lattice of two-atom base, the basis vectors are (0 0 0) and $(\frac{\vec{a}_1}{3}+\frac{\vec{a}_2}{3})$; where we define the triangular lattice's (basal) vectors a_1 and a_2, with $a_0 = 1.42\sqrt{3}$Å.

$$\begin{aligned} \vec{a}_1 &= a_0\ (\cos(+\frac{\pi}{6})\hat{\imath} \quad \sin(+\frac{\pi}{6})\hat{\jmath} \quad 0\hat{k}) \\ \vec{a}_2 &= a_0\ (\cos(-\frac{\pi}{6})\hat{\imath} \quad \sin(-\frac{\pi}{6})\hat{\jmath} \quad 0\hat{k}) \end{aligned} \tag{6.1}$$

6.2.2 Graphite polytypes:

Graphite is multi parallel graphene layers stacked one above another at distance 3.35Å. Carbon atoms in adjacent graphenes interact weakly by van der Walls interlayer interactions balanced with the electrostatic and quantum fermi repulsion between electrons in the completely full delocalized π molecular orbitals. Henceforth, the weakly bound layers are far apart and can slide one over another, describing thus why graphite is lubricant. Even though the (abab) hexagonal stacking of layers is the best arrangement reducing the inter-distance repulsion [16], natural and laboratory graphite crystalline contains 80% and 14% hexagonal and rhombohedral graphite respectively, where the 6% left is disordered. The three distinct graphite crystals, described later, can be completely distinguished by the hexagonal lattice basal vectors $\vec{a}_1$ and $\vec{a}_2$ in Eq.(6.1), and the following principal axis

$$\vec{a}_3 = pc_0\ (0\ 0\ \hat{k}) \tag{6.2}$$

with c_0 being equal to the interlayers' distance (3.35Å), and p is the periodicity along $\vec{a}_3$.

Simple hexagonal graphite

Simple hexagonal graphite, Fig.(6.3), is an example of graphite intercalation compounds, i.e., another element than carbon is intercalated (inserted) between graphene sheets that are located directly on the top of each other, i.e., (aaa) sequence. This crystal structure is described using the hexagonal lattice vectors $\vec{a}_1$ and $\vec{a}_2$ from Eq.(6.1), and $\vec{a}_3$ from Eq.(6.2)

with periodicity, ($p = p_s = 1$). Using the simple hexagonal lattice of one-atom bases at the origin, i.e. basis vector equals 0, the lattice of the simple hexagonal graphite is then viewed as two interpenetrating simple hexagonal lattices, with one translated by $(\frac{\vec{a}_1}{3} + \frac{\vec{a}_2}{3})$ from the other.

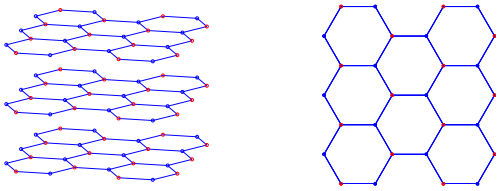

(a) Sideview (b) Topview.

Figure 6.3: Simple hexagonal Graphite

Hexagonal or Bernal graphite

Hexagonal graphite, Fig.(6.4), is the ground state of all carbon structures. Graphene Layers in this crystal adopt the (*abab*) stacking sequence: half the carbon atoms in one graphene lies midway in the line between those in the very two adjacent graphenes above and beneath, while the other half of carbons in the same plane lies midway in the line between the centers of the hexagons in the first two adjacent bounding planes.

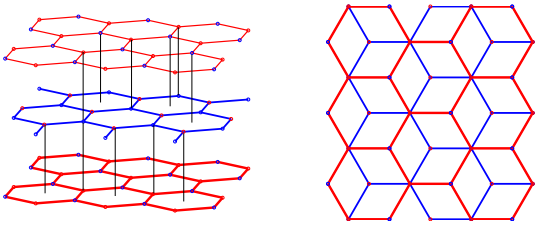

(a) Sideview (b) Topview.

Figure 6.4: Hexagonal Graphite

Bernal graphite lattice can be defined as two interpenetrating simple hexagonal graphite lattices whose vectors are now $\{\vec{a}_1,\ \vec{a}_2,\ \vec{a}_3\}$, $p = p_h = 2$; one of the simple hexagonal graphite lattice is shifted by $(\frac{\vec{a}_1}{3} + \frac{\vec{a}_2}{3} + \frac{\vec{a}_3}{2})$ from the other. In terms of the hexagonal lattice, i.e. an (abab) sequence of two close-packed layers with a relative translation $(\frac{\vec{a}_1}{3} + \frac{\vec{a}_2}{3} + \frac{\vec{a}_3}{2})$; the hexagonal graphite is formed by two hexagonal lattices placed at the origin

and $(\frac{\vec{a}_1}{3} + \frac{\vec{a}_2}{3})$.

Rhombohedral graphite

Rhombohedral graphite, Fig.(6.5), can not be isolated in a pure form, but found usually in small quantities in graphite crystals. Here graphene sheets have an (*abc*) extended stacking fault in the hexagonal system: half the carbon atoms in one graphene lies midway in the line between atoms in the graphene above and the centers of the hexagons in the graphene beneath, the other half of carbons in the same plane lies midway in the line between the centers of the hexagons in the above graphene and atoms in the graphene beneath.

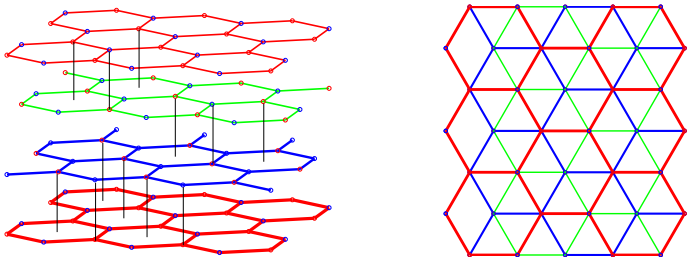

(a) Sideview (b) Topview.

Figure 6.5: Rhombohedral Graphite

The resultant lattice is interpreted by three interpenetrating simple hexagonal graphite lattices whose vectors are $\{\vec{a}_1,\ \vec{a}_2,\ \vec{a}_3\};\ p = p_r = 3$. The three simple hexagonal graphite lattices are located at the origin, $(\frac{\vec{a}_1}{3} + \frac{\vec{a}_2}{3} + \frac{\vec{a}_3}{3})$ and $(\frac{2\vec{a}_1}{3} + \frac{2\vec{a}_2}{3} + \frac{2\vec{a}_3}{3})$. The rhombohedral lattice is a stretched cubic close-packed lattice along the direction of a_3, and has three close-packed layers in (abc) sequence with two translated relative to the third by $(\frac{\vec{a}_1}{3} + \frac{\vec{a}_2}{3} + \frac{\vec{a}_3}{3})$ and $(\frac{2\vec{a}_1}{3} + \frac{2\vec{a}_2}{3} + \frac{2\vec{a}_3}{3})$. Rhombohedral graphite is equivalently two interpenetrating rhombohedral (elongated close-packed lattice), one translated from the other by $(\frac{\vec{a}_1}{3} + \frac{\vec{a}_2}{3})$.

6.2.3 Diamond polytypes

Diamond structure is a highly ordered network of tetrahedrally coordinated atoms, e.g carbon, silicon, or molecules as in water-ice. The intrinsic tetrahedral geometrical symmetry in diamond is attributed to the quadrivalent, tetravalent, sp^3-hybridized carbon or silicon atoms where each is covalently bonded to four other in the tetrahedral configuration, i.e any bond angle is approximately 109.4°. In water-ice structures, each water molecule is linked

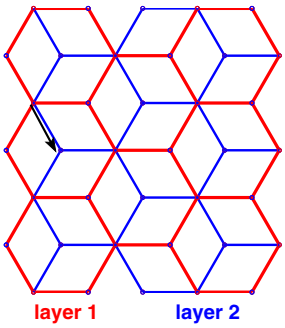

(a) Basal shift between layers 1 and 2

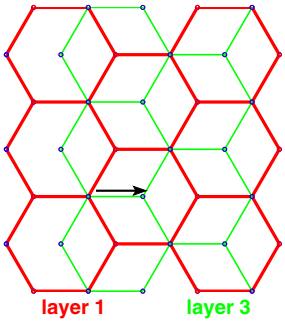

(b) Basal shift between layers 1 and 3

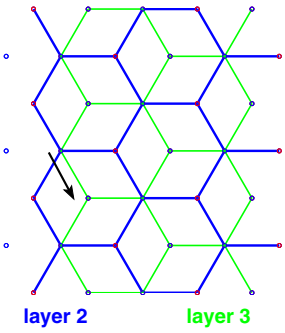

(c) Basal shift between layers 2 and 3

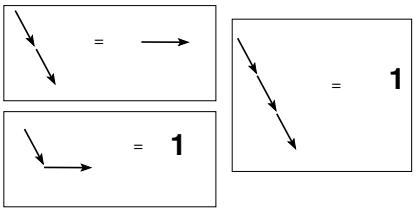

(d) Layers' basal shift arithmatics.

Figure 6.6: Basal shift in graphite layers

to four others by tetrahedrally oriented hydrogen bonds. There are mainly two diamond crystals reflecting the local tetrahedral symmetry, nevertheless they reflect different overall symmetries depending on how tetrahedrons are oriented relative to each other. Cubic diamond lattice results when each two tetrahedra are in the staggered configuration, i.e they contact one another in a vortex-to-vortex manner, their point of contact lies in the line joining their centers, and one's base is 60° rotated relative to the other's. The other crystal is the hexagonal diamond, it has both staggered and eclipsed configurations, the eclipsed configuration of two tetrahedra is when their bases eclipse one another. Naturally, diamond adopts both cubic and hexagonal lattices which are referred to herein as diamond and lonsdaleite (one element analogue of the wurtzite structure). At room temperature carbon diamond is mostly found in the energetically favored cubic form while the wurtzite structure is preferred at higher temperatures. Water-ice is a similar analogue such that the wurtzite structure occurs at temperatures above ($-80°$) whereas the cubic forms is most likely to occur at temperatures between ($-130° \rightarrow -80°$). Diamond and lonsdaleite relate one another by the same way hexagonal and cubic close-packed structures are related, as we shall soon describe. Hexagonal and cubic close packing are the most frequent stacking sequences, yet are they the only naturally existing. Intermixed stacking sequences of both are also adopted in nature. Such stacking fault, interrupted sequence, results in transforming a hexagonal to another bigger cubic or hexagonal lattice and vice versa [14, 35]. Analogous to the close-packed intermix, different synthesized diamond polytypes have layers in an alternate stacking sequences between diamond and lonsdaleite, as will be described later, and the new intermixed lattice exploits either the hexagonal or cubic symmetry. One of the many examples on such synthesized lattices is known as rhombohedral diamond which is just a larger hexagonal lattice. Throughout the remaining of this chapter, I will assume a familiarity of the reader with the close-packing schemes, otherwise extensive details on this topic and the types of lattices are found in [3, 18, 19, 35]. Different intermixed diamond lattices are described in [31, 48], and [29] provides some structural and mechanical properties of diamond polytypes.

To describe and show differences between the hexagonal and cubic lattices of diamond, we will use the regular tetrahedral proportions; considering a regular tetrahedron of side length L, then its center-to-vortex distance, R, is $\frac{1}{4}\sqrt{6}L$ and its height, H, is $\frac{1}{3}\sqrt{6}L$, and the distance from the center of any base to the tetrahedron center, r, is $\frac{1}{12}\sqrt{6}L$. The basal vectors defined in Eq.(6.1) have a length ($a_0 = L$), whereas a_3 is redefined by setting ($c_0 = H$) in Eq.(6.2), and cubic lattice periodicity is ($p_d = 3$), and that of lonsdaleite lattice is ($p_l = 2$).

Cubic diamond

A six close-packed layer repeat builds up diamond structures, Fig(6.7), those layers are not equidistant as in graphite, instead there are two interlayer distances characterized by the center-to-vortex distance,R, and the base center to the tetrahedron center, r. We view diamond lattice as two interpenetrating cubic packed lattices; one has the relative translation ($R\hat{a}_3 \equiv \frac{R}{p_d H}\vec{a}_3$). The ratio ($\frac{R}{3H}$) being equal to ($\frac{1}{4}$) with $|\vec{a}_3|$ representing the cubic cell diagonal, explains the description of the cubic diamond lattice by Kathlene Lonsdale[20]:

> *"... consists of two interpenetrating face-centered cubic patterns, separated from each other by a translation of a quarter of the cube diagonal ..."*

In the field of crystallography and mineralogy, this lattice is viewed as cubic close-packing of pyramids, i.e., a four-atom group where three are placed at the vortices of the regular tetrahedron and at its center lies the fourth atom. The close-packed layers of pyramids, i.e., bilayers of atoms where the two layers are separated by the distance $r = \frac{1}{12}\sqrt{6}L$, are known as buckled layers or buckled graphenes sometimes, and are used to describe the layers' relative shift.
The unit cell of the hexagonal system is usually considered to be a right rhombic prism which is $\frac{1}{3}$ of the hexagonal prism and it is itself a parallelepiped. While a right rhombic prism can be recognized as translational unit repeat for diamond, it can not represent its space group symmetry; diamond is known to have four 3-fold axes of symmetry which proceed diagonally from corner to corner through the center of the cube which is conventionally taken as a unit cell of diamond.

Hexagonal diamond "lonsdaleite"

Lonsdaleite lattice, Fig(6.8), is a construction of a non-equidistant four close-packed layer repeat, the interlayer distances are the same as in diamond. The whole structure is formed by two hexagonal close-packed cells interpenetrating each other at ($R\hat{a}_3 \equiv \frac{R}{p_l H}\vec{a}_3$). Two different bilayers occur in lonsdaleite, they can not be described only by translation but either by a reflection or a combined translation and rotation; that is to say: it is impossible to have hexagonal close-packed tetrahedra (pyramids) if we are to preserve their orientations. In other words, hexagonal close-packing requires objects to have a bilateral "mirror" symmetry along the principal axis.

With reference to Figs.(6.7 and 6.8), the major difference between those two tetrahedrally symmetric structures is the four-atom configuration or dihedral conformation as used in

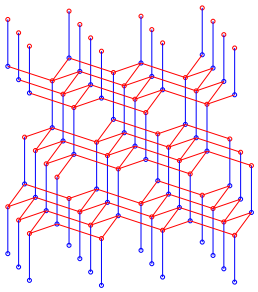

(a) Sideview

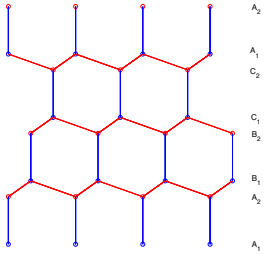

(b) Layers stacking sequence

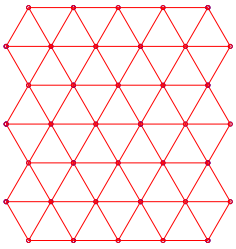

(c) Topview.

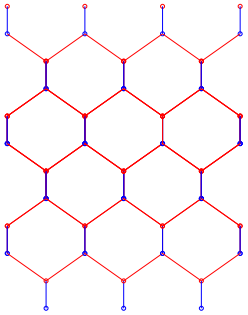

(d) Sideview.

Figure 6.7: Cubic Diamond

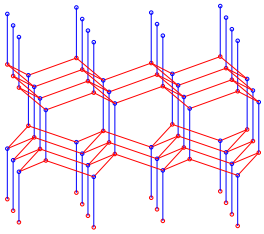

(a) Sideview

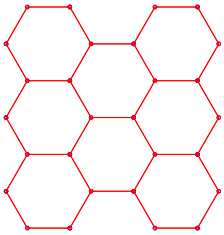

(b) Topview.

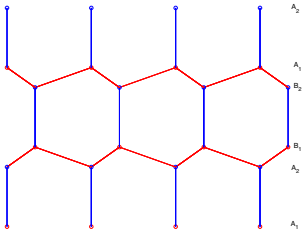

(c) Layers stacking sequence.

Figure 6.8: Lonsdaleite, the hexagonal diamond

chemistry. Dihedral configuration in diamond is either $\frac{\pi}{3}$, π or $\frac{5\pi}{3}$, where lonsdaleite has zero-, $\frac{2\pi}{3}$ $\frac{4\pi}{3}$ dihedral angles. This difference is reflected in two different chain types, Fig.(4.4), and two different six-membered buckled rings. Following the series of 180-dihedral angle reveals the aliphatic chain which does occur in both diamond and lonsdaleite. The "armchair" chain occurs only in lonsdaleite, and is described when we follow both the zero- and 180- torsional angles successively. Each atom in diamond is common to six aliphatic chains whereas an atom in lonsdaleite is common to three chains of each type. The smallest closed circuits of the bonded atoms are the buckled hexagonal rings[21], diamond has only one type of rings that correspond to a series of 60° dihedral angles (staggered configuration of any two tetrahedra), it is ofcourse the familiar ring of chair configuration. Lonsdaleite has, in addition to the six-membered chair-configuration rings, six-membered rings in the boat configuration, i.e., a ring which possess four 60°- and two 0°- torsional angles.

6.2.4 Tetrahedral model to build up diamond structures

In accordance to our orbital based representation of atoms, Sec.(7.3), for molecular dynamics, the sp^3 hybridized atom is represented by an atomic center with prescribed geometric arrangement of active orbitals, represented by four equivalent arms pointing to vortices of a regular tetrahedron, the length of each arm is half length the σ-bond in diamond structure. Orientations of arms indicate the best directions in space for covalent interactions. There exist tools, see Fig.(6.9), with similar representation to build up and view many complicated structures. The first of the tool sets we have used, is the "Orbit molecular building system" which comprises one-, two-, three-, four-, up to twelve-pronged atomic centers. The second set was the "Organichem model set", which comprises only one-, three-, and four-pronged atomic centers, making it good enough to build up structures of graphene, diamond and lonsdaleite. Those two sets were of a great help to visualize such complicated structures. Other visualization tools were the VMD and JMOL as indicated in the introduction.

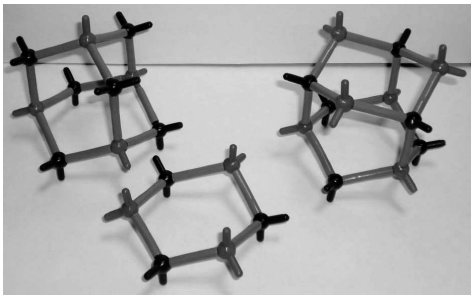

Shown furthest left the so-called carbon cage in cubic diamond, furthest right is the carbon cage of lonsdaleite, and at the middle is the non-planar hexagon known as buckled or puckered hexagon, or simply the hexagon in the chair configuration.

Figure 6.9: Tool sets

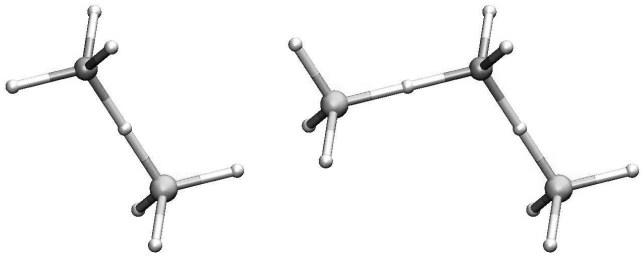

Figure 6.10: Visualization in VMD and Jmol

To build up diamond and lonsdaleite structures with emphasis on their tetrahedral symmetry, tetrahedra are packed into one hexagonal basal layer. In that sense, two arms (one per tetrahedron) touch each other at their outer edges and get aligned in a straight line (presenting the bond), then tetrahedra are rotated 60°, around their common axis (bond), relative to each other (staggered configuration). Keeping on so doing, results in a common layer for both structures. Diamond is completely determined by four layers, where all first neighboring tetrahedra in whatsoever direction are in the staggered configuration. For the second layer in lonsdaleite, one tetrahedron is packed along the principal axis and is oriented in the eclipsed configuration with one tetrahedron in the first layer. To continue, keep on so doing as long as you are in the direction of the principal axis, or you can do what has been done earlier to build up the first layer, the same is repeated to get lonsdaleite structure which is determined by three of such layers.

Using layers' stacking as a common ground for analogy and comparison between both structures, we construct four similar basal layers. In lonsdaleite, each layer is a mirror reflection of the one beneath, i.e., flip the second layer up-side-down and stack it upon the first, the third layer would also be a mirror reflection of the second, and is simply identical to the first. To get diamond, flip the second layer, rotate it 60 degrees around one bond parallel to the principal axis and stack it upon the first, flip the third layer that was completely congruent to the second, rotate around one bond 60 degrees in the same direction of the first rotation, and stack it. The fourth is 60 degrees rotated reflection of the third, which would be equivalent to the first. Remember bilayers in diamond can be stacked only by proper translations as was earlier explained.

Intermixed diamond crystals can be built up by stacking such bilayers, i.e., alternate flipped (reflected) and rotated flipped layers in the proper sequences. For details on some of the possible sequences and their corresponding unit cells, the reader is referred to [31, 48]. The h-c notation is usually used in crystallography and can be found here [19]. In the h-c notation, each layer is specified in terms of the orientation of layers above and beneath. 'h' stands for a hexagonally stacked layer, i.e., surrounded on either side by two layers in

similar orientation. 'c' denotes a layer in cubic configuration, i.e., surrounded on either side by layers in different orientations. One example is the structure that has an (abcacb) stacking sequence, and can be written as (hcchcc) in the h-c notation, while (abacacbcb) stacking is described as hhc.

6.2.5 Phase transition between carbon allotropes

The formation of diamond from graphite can be achieved through application of high temperatures and high pressure. Such transition are difficult to control. Recently, as described in ref.([32]), femtosecond laser pulses have been used to induce the formation of diamond from graphite. The process has been monitored at the crystal structure level by ultrafast electron crystallography.

Chapter 7

Introduction to papers

The following papers are submitted as part of this thesis:

1. L. Kocbach and S. Lubbad (2009), *Reactive interatomic potentials and their geometrical features*

   being submitted to Modelling and Simulation in Materials Science and Engineering

2. S. Lubbad and L. Kocbach (2009), *Exploring molecular dynamics with forces from n-body potentials using Matlab*

   being submitted to Computer Physics Communications

3. L. Kocbach and S. Lubbad (2009), *Design of Orbital Based Molecular Dynamics Method*

   being submitted to Modelling and Simulation in Materials Science and Engineering

4. L. Kocbach and S. Lubbad (2009),

   Transverse dipole-dipole effective interaction for sheet arrangements

   A short letter, submitted tentatively to Physical Review Letters

5. L. Kocbach and S. Lubbad (2009),

   Geometrical simplification of the dipole-dipole interaction formula

   submitted to Physics Education

The papers are shortly presented in the following sections

7.1 Reactive interatomic potentials and their geometrical features

A large number of simulations is based on the so called bond-order potentials, mainly the Tersoff and Brenner versions. These potentials are highly empirical, based originally on the concept of bond order, i.e. the presence of other atoms (bonds) influences the strength of the individual terms of the potential. The potential energy, giving rise to the individual forces, assumes a full summation over all of the constituents, in practice limited by the cut-off properties of the model.

From some recent papers a reader might get the impression that the empirical potentials are no longer necessary because the advances in computing will soon allow quantum mechanical calculations of atomic interactions based on e.g. density functional methods for nearly any type of atomic scale simulations. This work shows, among other things, that the empirical potentials are still used in many applications and will probably remain to be used for studies of some aspects of particle systems for a long time. The project reported here started as a simple investigation of how do the Tersoff-Brenner potentials model the geometrical or stereochemical features of the modeled aggregates of atoms. During this work we found details about a number of alternative approaches and the comparisons between the various features lead us to the presented analysis.

These results should be useful for researchers starting work on various molecular structures of the type covered by any of the mentioned approaches to atom-atom interactions, as well as for projects aiming at development of improved or combined systems. In this thesis the work described in section 7.3 could not be carried out without this comparative study. In the paper we discuss the models known as EDIP, ABOP, ReaxFF as well as *ab initio* methods, and two special features, use of neural networks on one side and synthetic diamond-like structures from elements interacting by two-body isotropic potentials.

7.2 Exploring molecular dynamics with forces from n-body potentials using Matlab

As the title of this paper indicates, it is concerned with our method to explore the evaluation of forces from n-body potentials using the matrix-oriented system MATLAB. The classical Newtonian equations of molecular dynamics (MD) can be solved using the Verlet algorithm, which makes the programing rather short and simple. An important feature, discussed below is that MATLAB allows to write element-wise operations on complex objects (vectors, matrices, multidimensional arrays) as if they were simple numbers. In the paper we have

described methods which can be useful in design and exploration of new methods, or simply in education. While the large systems require optimization of the computations and often possibility of parallel computation, the presented MD models are supposed to be of the size up to tenths or possibly hundreds of particles. We show that for such relatively small systems of model atoms the computations can be carried out inside the systems MATLAB (or OCTAVE).

It is generally well known that MATLAB and related systems have interpreted programming languages, which make execution of large programs rather slow. On the other hand, they have the ability to perform mathematical operations on complicated structured objects in one single statement using ordinary mathematical notation. This property is essential for our approach. A simple MD simulation code with pair potentials can be written in about 30 statements. These can be complemented by another set of routines of a comparable size (about 20 to 30 statements) for quite powerful real time visualizations.

It should be mentioned that similar types of operations can be designed in Object Oriented programming methodology, but the simplicity of MATLAB and OCTAVE together with the built in visualization techniques can not be matched by any general purpose programming languages and libraries, perhaps with the exception of the libraries for the language python (SciPY - Scientific Python and pylab - an analogue to MATLAB)

7.3 Design of Orbital Based Molecular Dynamics Method

This paper presents a proposal of a rather new type of effective interatomic interaction for molecular dynamics and similar applications. It introduces the concept of Orbital-Based Molecular Dynamics interactions (OBMD). The model consists of atoms with prescribed geometric arrangement of active orbitals, represented by arms of the length of half of the relevant bond lengths. The interactions have a repulsive part between the atomic centers and an attraction between the arm ends of different atoms. For each atom pair only the closest pair of arms interacts attempting to form the bond. This is a picture of sigma bonds, the pi bonds are modeled by alignment of additional internal vectors which might characterize a given atom. Also these are primarily pair interactions. Thus there are only pair interactions of several types present. The intrinsic arrangement of the model elements, virtual orbitals, or arms and internal vectors can be switched depending on the environment. Thus the complexity of the many-body potentials is replaced by pair interactions between atoms with complex internal behavior. The proposed model thus allows formation of new geometries, establishing new and breaking existing bonds with the use of only pair interactions and environment scanning. The switching of the bond

character is supposed to be implemented as stochastic quantum jumps with probabilities determined by the local environment (coordination number, i.e. a function of the number of closest neighbors). SUch features already exist in some of the models described in the paper of section 7.1.

The rigid character of the geometrical structures requires their re-orientation by rotational motion to get the right orientation of mutually interacting atoms. Since the unoptimized orientation of the arms can not represent a physically relevant energy of the system, the rotational arrangement is modeled as rotation of over-damped type, in analogy to the Langevin dynamics. The unphysical excitation energy is thus dissipated to unphysical friction and is automatically removed from the system. In contrast to that, the relative displacements of the arms and their imperfect angular alignment are parts of the physical model and the resulting potential energies and forces become the physically important part of the model.

We discuss in some detail the carbon case and very shortly also hydrogen, silicon and sulfur. Determination of detailed values of the model parameters is not attempted at this stage. Most of the parameters can be extracted from the existing models reviewed in section 7.1. This is relatively a simple task, since only pair interactions are present.

7.4 Transverse dipole-dipole effective interaction for sheet arrangements

In this short letter we propose a simple effective interaction which can be tuned to arrange the interacting objects into sheets. The interaction is based on the decomposition of the dipole-dipole interaction into two components, one parallel and one perpendicular to the connecting line between the dipoles. A very detailed discussion of this decomposition can be found in the work described in 7.5 Only the perpendicular part is used here. Various aspects of this simple interaction are discussed, in particular in connection to two recent papers on self assembly of carbon nanostructures. On the other hand, the features discussed are quite general and might be of interest in different areas of microscopic modeling.

In this thesis, the work in 7.3 uses also this form as one part of a much more complex model.

7.5 Geometrical simplification of the dipole-dipole interaction formula

The well known formula for dipole-dipole interaction potential energy is well known. For our purpose we needed to work with simple representations and thus the idea presented here seemed suitable for a more popular presentation. This was especially motivated by the fact that we have by chance found small magnets which added some extra fun to the presentation. At different levels of their education students of both chemistry and physics are exposed to the presentation of dipole-dipole potential energy when they are taught electrostatics or magnetostatics. This popular formula is also featured in the encyclopedias.

We have shown that by a simple rewriting of the formula it becomes apparent that for example, by reorienting the two dipoles, their attraction can become exactly twice as large. The physical facts are naturally known, but the presented transformation seems to underline the geometrical features in a rather unexpected way. The consequence of the discussed features is the so called magic angle which appears in many applications. We also discussed possibility for designing educational toys based on small magnets. Finally, we have tried to to understand why this formula has not been written down frequently before this work. Similar transformation is possible for the field of a single dipole, there it seems to be observed earlier, but also in this case we could not find any published detailed discussion.

This popular science paper complements the other papers, since we have based the two model interactions of section 7.3 (OBMD model) and section 7.4 (TDDI model) on a part of the dipole-dipole expressions which otherwise probably would not be designed in this simple way.

Chapter 8

Conclusion

We believe that the empirical model interactions with pre-defined potential functions will remain an important tool of molecular modeling even though the more fundamental or *ab initio* methods are becoming more and more attractive with the development of computing facilities. Therefore I feel that the presented work aimed at increased understanding and knowledge of a class of both previously available empirical approaches and the proposed extensions is a relevant contribution to the some areas of molecular modeling.

For an adequate modeling of different molecular geometries consistent with experimental results there must be mechanisms represented by many body interaction leading to geometrical relations to which atoms in a larger system are known to adapt themselves. We have seen that the three-body interaction is the simplest necessary contribution used in many applications. However, we have seen that in the case of tetrahedral structures there is a problem of modeling the so called cubic and hexagonal polytypes (section 6.2.3) with the three-body approach alone. In this case all the three-body correlations are exactly the same, but the over all crystal structure is drastically different. It means that in this case the four-body correlations in terms of the so called dihedral angle must be included in the modeling to account for the difference. Inclusion of four-body and higher interactions is of course a matter of complexities both in parameterizations and data fitting, also the computational cost would be considerably increased.

We have shown that the four-body correlations may be included explicitly in the interaction forms or implicitly by relying on the basic topological properties of the Euclidean space. The implicit approach is not limited to the four-body case. In section 4.2.3 I have explained that with the Tersoff or already Stillinger-Weber type of three-body correlation one obtains diamond-like structures in the three-dimensional space, hexagonal sheet in the two-dimensional Euclidean space and the C_{60} fullerenes on the sphere.

Finally, I would like to stress our proposal of Orbital Based Molecular Dynamics method

(OBMD). This simple and intuitive model requires only a set of pair-interactions, and is capable to generate various structures with less parameters, data fitting and computational costs. Moreover, it is proposed to involve environment dependence, where each atom itself configures its own orbitals in response to the presence of bonding neighbors, i.e. a geometrical re-structurabilty is part of the model atom.

The OBMD has only been described as a model without full specific implementation. A straight forward simple implementation could have been attempted by simply consulting the tables of bond lengths and strengths and then adjusting one of the simple functional forms to a subset of vibrational characteristics. However, we think that such a simple implementation would not compete well with the already existing models, and that the full range of its possibilities could not be appreciated. We thus believe that a more thorough implementation, hopefully involving a much broader participation of collaborators will be performed in the future. This I believe is the main line of continuation of the present project.

Further possible extensions to consider is the treatment of the other directional interactions of hydrogen bonding in a very similar procedure. According to the usual picture, hydrogen bonding would involve interactions between two nonbonded atoms of different types such that the positive center on one atom and one negative center representing the so-called lone-pair orbital on the other atom. We have recently found a paper arguing for covalency of the hydrogen bonding [15], involving basically the three instead of just two atoms. It would be very interesting to perform the quantum chemical calculations and try to develop a similar model as the OBMD above for the hydrogen bonding, in the way indicated in the last quoted paper. Alternatively, one could also try to be formulate a two-body interaction in a similar way as discussed in papers 3 and 4 which are attached to this thesis.

Bibliography

[1] G. C. Abell. Empirical chemical pseudopotential theory of molecular and metallic bonding. *Phys. Rev. B*, 31(10):6184–6196, May 1985.

[2] Michael P. Allen. Introduction to molecular dynamics simulation. In Helmut Grubmüller Kurt Kremer Norbert Attig, Kurt Binder, editor, *Computational Soft Matter: From Synthetic Polymers to Proteins, Lecture Notes*, volume Vol 23 of *NIC Series*, pages 1–28. John von Neumann Institute for Computing, Jülich, 2004.

[3] Ashcroft and Mermin. *Solid state physics*. Harcourt, Inc., 1976.

[4] B. M. Axilrod and E. Teller. Interaction of the van der waals type between three atoms. *The Journal of Chemical Physics*, 11(6):299–300, 1943.

[5] B. H. Bransden and C. J. Joachain. *Physics of atoms and molecules*. Longman Scientific & Technical, second edition, 1983.

[6] Donald W. Brenner. Relationship between the embedded-atom method and tersoff potentials. *Phys. Rev. Lett.*, 63(9):1022, Aug 1989.

[7] Donald W. Brenner. Empirical potential for hydrocarbons for use in simulating the chemical vapor deposition of diamond films. *Phys. Rev. B*, 42(15):9458–9471, Nov 1990.

[8] Donald W Brenner, Olga A Shenderova, Judith A Harrison, Steven J Stuart, Boris Ni, and Susan B Sinnott. A second-generation reactive empirical bond order (rebo) potential energy expression for hydrocarbons. *Journal of Physics: Condensed Matter*, 14(4):783–802, 2002.

[9] R. Car and M. Parrinello. Unified approach for molecular dynamics and density-functional theory. *Phys. Rev. Lett.*, 55(22):2471–2474, Nov 1985.

[10] Nikos L. Doltsinis. Molecular dynamics beyond the born-oppenheimer approximation: Mixed quantum-classical approaches. In D.Marx J. Grotendorst, S. Bluügel, editor,

Computational Nanoscience: Do it yourself, volume Vol 31 of *NIC Series*, pages 389–409. John von Neumann Institute for Computing, Jülich, 2006.

[11] J. H. Dymond and B. J. Alder. Pair potential for argon. *The Journal of Chemical Physics*, 51(1):309–320, 1969.

[12] Furio Ercolessi. A molecular dynamics primer. 1997.

[13] Eduardo HL Facao and Fred Wudl. Carbon allotropes: beyond graphite and diamond. *Journal of Chemical Technology and Biotechnology*, 82:524–531, February 2007.

[14] Christopher Hammond. *The Basics of Crystallography and Diffraction*, pages 5–9. Oxford University Press, second edition, 2001.

[15] E. D. Isaacs, A. Shukla, P. M. Platzman, D. R. Hamann, B. Barbiellini, and C. A. Tulk. Compton scattering evidence for covalency of the hydrogen bond in ice. *Journal of Physics and Chemistry of Solids*, 61(3):403 – 406, 2000.

[16] X. Gonze J. C. Charlier and J.P. Michenaud. Graphite interplanar bonding: Electronic delocalization and van der waals interactions. *EUROPHYSICS LETTERS*, 28(6):403–408, 1994.

[17] João F. Justo, Martin Z. Bazant, Efthimios Kaxiras, V. V. Bulatov, and Sidney Yip. Interatomic potential for silicon defects and disordered phases. *Phys. Rev. B*, 58(5):2539–2550, Aug 1998.

[18] Charles Kittel. *Introduction to Solid State Physics*. Jone Wiley & Sons, Inc, seventh edition, 1996.

[19] P. Krishna and D. Pandey. Closed-packed structures. University College Cardiff Press for the International Union of Crytallography, 2001.

[20] Kathleene Lansdale. Diamonds, natural and artificial. *Nature (London)*, 153:669–672, June 1944.

[21] Kathleene Lansdale. Formation of lonsdaleite from single crystal graphite. *The american Mineralogist*, 56:333–336, January-february 1971.

[22] Nikos L.Doltsinis and Dominik Marx. First principles molecular dynamics involving excited states and nonadiabatic transitions. *Journal of Theoretical and Computational Chemistry (JTCC)*, 1(2):319–349, 2002.

[23] Andrew R. Leach. *Molecular Modelling, principles and applications*. Pearson Prentice -hall, second edition, 2001.

[24] Jianhui Li, Zhongwu Zhou, and Richard J. Sadus. Modified force decomposition algorithms for calculating three-body interactions via molecular dynamics. *Computer Physics Communications*, 175(11-12):683 – 691, 2006.

[25] Gianluca Marcelli. *The Role of Three-Body Interactions on the Equilibrium and Non-Equilibrium Properties of Fluids from Molecular Simulation.* PhD thesis, Centre for Molecular Simulation and School of Information Technology, Swinburne University of Technology, 2001.

[26] N. A. Marks. Generalizing the environment-dependent interaction potential for carbon. *Phys. Rev. B*, 63(3):035401, Dec 2000.

[27] Dominik Marx and Jürg Hutter. Ab initio molecular dynamics: Theory and implementation. In Johannes Grotendorst, editor, *Modern Methods and Algorithms of Quantum Chemistry, Proceedings*, volume Vol 3 of *NIC Series*, pages 329–477. John von Neumann Institute for Computing, Jülich, 2000.

[28] Stephan Knapek Michael Griebel and Gerhard Zumbusch. *Numerical Simulation in Molecular Dynamics, Numerics, Algorithms, Parallelization, Applications.* Springer, 2007.

[29] Kazuhisa. Miyoshi and Lewis Research Center. *Structures and mechanical properties of natural and synthetic diamonds [microform] / Kazuhisa Miyoshi.* National Aeronautics and Space Administration, Lewis Research Center ; National Technical Information Service, distributor, [Cleveland, Ohio] : [Springfield, Va. :, 1998.

[30] K. S. Novoselov, A. K. Geim, S. V. Morozov, D. Jiang, Y. Zhang, S. V. Dubonos, I. V. Grigorieva, and A. A. Firsov. Electric Field Effect in Atomically Thin Carbon Films. *Science*, 306(5696):666–669, 2004.

[31] C. Raffy, J. Furthmüller, and F. Bechstedt. Properties of hexagonal polytypes of group-iv elements from first-principles calculations. *Phys. Rev. B*, 66(7):075201, Aug 2002.

[32] Ramani K. Raman, Yoshie Murooka, Chong-Yu Ruan, Teng Yang, Savas Berber, and David Tománek. Direct observation of optically induced transient structures in graphite using ultrafast electron crystallography. *Physical Review Letters*, 101(7):077401, 2008.

[33] D.C Rapaport. *The art of molecular Dynamics simulation.* Cambridge university press, first edition, 1995.

[34] Mikael C. Rechtsman, Frank H. Stillinger, and Salvatore Torquato. Synthetic diamond and wurtzite structures self-assemble with isotropic pair interactions. *Physical Review E (Statistical, Nonlinear, and Soft Matter Physics)*, 75(3):031403, 2007.

[35] Lesley Smarth and Elaine Moore. *Solid State Chemistry*. Stanley Thornes (Publishers) Ltd, second edition, 1998.

[36] Frank H. Stillinger and Thomas A. Weber. Computer simulation of local order in condensed phases of silicon. *Phys. Rev. B*, 31(8):5262–5271, Apr 1985.

[37] J. V. Sumanth, David R. Swanson, and Hong Jiang. A symmetric transformation for 3-body potential molecular dynamics using force-decomposition in a heterogeneous distributed environment. In *ICS '07: Proceedings of the 21st annual international conference on Supercomputing*, pages 105–115, New York, NY, USA, 2007. ACM.

[38] Ian Ivar Suni. Effect of three-body dispersion interactions on the surface dynamics of ar(111). *Surface Science*, 391(1-3):L1212 – L1216, 1997.

[39] Godehard Sutmann. Molecular dynamics - vision and reality. In D.Marx J. Grotendorst, S.Bluügel, editor, *Computational Nanoscience: Do it yourself*, volume Vol 31 of *NIC Series*, pages 159–194. John von Neumann Institute for Computing, Jülich, 2006.

[40] J. Tersoff. New empirical model for the structural properties of silicon. *Phys. Rev. Lett.*, 56(6):632–635, Feb 1986.

[41] J. Tersoff. Empirical interatomic potential for carbon, with applications to amorphous carbon. *Phys. Rev. Lett.*, 61(25):2879–2882, Dec 1988.

[42] J. Tersoff. New empirical approach for the structure and energy of covalent systems. *Phys. Rev. B*, 37(12):6991–7000, Apr 1988.

[43] J. Tersoff. Modeling solid-state chemistry: Interatomic potentials for multicomponent systems. *Phys. Rev. B*, 39(8):5566–5568, Mar 1989.

[44] John S. Tse. Ab initio molecular dynamics with density functional theory. *Annual Review of Physical Chemistry*, 53(1):249–290, 2002.

[45] Jan van Ruitenbeek. Atomic wires of carbon. *Physics*, 2:42, May 2009.

[46] Loup Verlet. Computer "experiments" on classical fluids. i. thermodynamical properties of lennard-jones molecules. *Phys. Rev.*, 159(1):98, Jul 1967.

[47] Hans H. Diebner Walter Nadler and Otto E. Rössler. Space-discretized verlet-algorithm from variational principle. *Z. Naturforsch*, 52a:585–587, 1997.

[48] Bin Wen, Jijun Zhao, Michael J. Bucknum, Pingkun Yao, and Tingju Li. First-principles studies of diamond polytypes. *Diamond and Related Materials*, 17(3):356 – 364, 2008.

[49] Nicholas Thomas Wilson. *The Structure and Dynamics of Noble Metal Clusters*. PhD thesis, School of Chemistry, University of Birmingham, September 2000.